Master's thesis

NTNU
Norwegian University of Science and Technology
Faculty of Engineering
Department of Civil and Environmental Engineering

Fredrik Nilsen Rochmann

Lateral Pile Group Effects

A Finite Element Study on the Effects of Pile Spacing and Loading Direction on the Lateral Bearing Capacity and Stiffness of Small Pile Groups

Master's thesis in Civil and Environmental Engineering

June 2020

NTNU
Norwegian University of
Science and Technology

Fredrik Nilsen Rochmann

Lateral Pile Group Effects

A Finite Element Study on the Effects of Pile Spacing and Loading Direction on the Lateral Bearing Capacity and Stiffness of Small Pile Groups

Master's thesis in Civil and Environmental Engineering
June 2020

Norwegian University of Science and Technology
Faculty of Engineering
Department of Civil and Environmental Engineering

NTNU
Norwegian University of
Science and Technology

Preface

This master thesis is submitted as a partial fullfillment of my MSc. degree in Civil and Environmental Engineering at the Norwegian University of Science and Technology (NTNU) in Trondheim. The thesis has been carried out in cooperation with the Norwegian Geotechnical Institute (NGI). All work for this thesis has been carried out in its entirety during the spring semester of 2020.

Trondheim, 2020-06-07

Fredrik Nilsen Rochmann

Acknowledgment

I acknowledge Dr. Youhu Zhang at NGI for proposing the topic of this thesis to me. I am very grateful to him for his continuous support and advice during the entirety of the semester. I also acknowledge the help of Yonqing Lai with the numerical modelling in ABAQUS.

F.N.R

Abstract

Jacket foundations are a widely used foundation type for offshore wind turbines and oil platforms. The jacket is a truss consisting of several legs that transfer the load to the seabed. Each leg is often supported by piles in order to provide sufficient bearing capacity and stiffness. The piles are typically used in groups of 2 to 4 closely spaced piles. Due to large wind and wave actions the piles must be designed for substantial lateral loading. Common practice is to model the piles as a Winkler foundation with corresponding p-y curves from relevant industry standards. The challenge is that the p-y curves are designed for isolated single piles. Because of pile-soil-pile interaction the bearing capacity and stiffness of a group-pile may be less than an equivalent isolated single pile. The p-y curves must therefore be modified to account for negative group effects. A numerical study of a flow-around failure for several 2-,3- and 4-pile group configurations is conducted in ABAQUS. The impact of two parameters, pile spacing (S/D = 2-5) and loading direction, on the group response is investigated. Reduction of ultimate bearing capacity and stiffness due to group effects is quantified in terms of group p- and y-multipliers. Functions for predicting the p- and y-multipliers based on the parameters is proposed for use in practical design situations. Depending on the pile group configuration the sensitivity of the multipliers to the two parameters varies. Group effects are generally largest for the closest pile spacing of S/D = 2 with a bearing efficiency in the range of 72 - 85 % of full capacity. As the pile spacing increase the negative group effects slowly diminish with bearing efficiency of 95-100 % for S/D = 5.

Sammendrag

En jacket er en vanlig benyttet fundamenttype for offshore vindmøller og plattformer. Jacketen består av et fagverk med flere bein som overfører laster til havbunnen. For å oppnå tilstrekkelig bæreevne og stivhet av fundamentet blir peler ofte benyttet. Pelegruppene består hovedsakelig av 2 til 4 peler med liten innbyrdes avstand. På grunn av store vind og bølgekrefter til havs må pelene prosjekteres for betydelig horisontal belastning. Vanlig praksis er å betrakte pelen som en Winkler-bjelke med tilhørende p-y kurver fra standarder. Utfordringen er at p-y kurvene er utformet for enkeltpeler og på grunn av pel-jord-pel interaksjon kan den horisontale bæreevnen og stivheten til en pel i en pelegruppe ofte være betydelig mindre enn for en tilsvarende frittstående pel. P-y kurvene utarbeidet for enkeltpeler må dermed modifiseres for å ta hensyn til negative effekter som oppstår i pelegrupper. I denne studien er det utført numeriske analyser av en «flow-around» bruddmekanisme for flere ulike pelegruppe konfigurasjoner i ABAQUS. Innvirkningen av to parametere, peleavstand og lastretning, på responsen av pelegruppen er undersøkt. Reduksjonen i bæreevne og stivhet er kvantifisert med p-og y-faktorer. Funksjonsuttrykk for å bestemme p- og y-faktorer basert på peleavstand og lastretning er utviklet for bruk i prosjekteringssammenheng. P- og y-faktorenes sensitivitet til de to faktorene er avhengig av pelekonfigurasjonen. Negative gruppe-effekter er generelt størst for en peleavstand S/D = 2 med en virkningsgrad fra 72 - 85 % av fullt utnyttet bæreevne. Virkningsgraden øker etter hvert som avstanden mellom pelene blir større og nærmest full bæereevne (95 – 100 % av total horisontal kapasitet) kan utnyttes for S/D = 5.

List of Figures

1.1 Jacket foundation with four legs 5

2.1 Failure modes for a laterally loaded pile (Jeanjean et al. (2017)) 9
2.2 Flow around mechanism for a fully rough pile (Randolph and Houlsby (1984) 9
2.3 Variation of N_p with depth for two soil profiles and pile diameters 12
2.4 Principle of a Winkler foundation (Karasin and Aktas (2014) 12
2.5 Modelling of the lateral pile response with p-y springs (Fayyazi (2015) 13
2.6 Relationship between the displacement, slope, bending moment, shear force and soil pressure of the pile (Reese and van Impe (2010) 15
2.7 A general p-y curve (Dodds and Martin (2007)) 15
2.8 Concept of scaling soil stress-strain curve to a p-y curve (Zhang and Andersen (2017)) 18
2.9 Lateral soil pressure on pile for different loading conditions (Pando et al. (2006)) 19
2.10 Shadow and edge effects in pile groups (Walsh (2005) 20
2.11 Pile group test load - deflection curve (Rollins et al. (2006)) 20
2.12 Concept of the y-multiplier (Dodds and Martin (2007)) 21
2.13 Bogard and Matlock's concept for generating group-pile p-y curves (Bogard and Matlock (1983)) 22
2.14 Concept of the p-multiplier (Dodds and Martin (2007) 23
2.15 P-multiplier from model and full scale tests for 3x3 pile groups (S/D = 3) in clay and sand 26
2.16 An equivalent pier defined from a 3-pile group 27

3.1 Finite element model of a 1 m soil and pile group slice 29
3.2 Analyzed pile group configurations 30
3.3 Element mesh 32
3.4 Computed single pile p-y curves from FE (full lines) and Zhang and Andersen (2017) (dashed lines) 33

4.1 Ultimate group capacity for different values of γ_{pf} 36
4.2 Group p-y curves computed from single pile p-y curves and actual group response for different γ_{pf} 37
4.3 2-pile group 38

4.4 Normalised p-y curves (S/D = 2,3,4,5). The red curve show the single isolated pile response 39
4.5 y-multiplier 2-pile group 39
4.6 Displacement contours for a single pile and 2-pile group with S/D = 1.25, 2 and 3 for $\omega = 90°$ 40
4.7 Proposed function for p_{mod} (dashed lines) vs FE results (dots) 41
4.8 Proposed function for y_{mod} (dashed lines) vs FE results (dots) 42
4.9 Comparison of p-multiplier with existing method 2-pile group. No gap 43
4.10 Comparison of p-multiplier with existing method 2-pile group. With gap 44
4.11 3-pile group (90 ° triangle 45
4.12 P-multiplier for 3-pile group (90 ° triangle) (S/D = 2,3,4,5) 45
4.13 y-multiplier 3-pile group (90° triangle) 46
4.14 Displacement contours for 3-pile group (90°) 47
4.15 Proposed function for p_{mod} (dashed lines) vs FE results (dots) 48
4.16 Proposed function for y_{mod} (dashed lines) vs FE results (dots) 49
4.17 Comparison of p-multiplier with existing method 3-pile group (90°) No gap 50
4.18 Comparison of p-multiplier with existing method 3-pile group (90°). With gap 51
4.19 3-pile group (equilateral triangle) 52
4.20 P-multiplier for 3-pile group (equilateral) (S/D = 2,3,4,5) 52
4.21 Functions for p- and y-multipliers (equilateral triangle) 53
4.22 Proposed function for p-mod vs FE results 54
4.23 Comparison of p-multiplier with existing method 3-pile group (equilateral). No gap 55
4.24 Comparison of p-multiplier with existing method 3-pile group (equilateral). With gap 56
4.25 3-pile group (120 ° triangle) 57
4.26 P-multiplier for 3-pile group (120 deg) (S/D = 2,3,4,5) 58
4.27 y-multiplier 3-pile group (120° triangle) 58
4.28 Displacement field for 120 degree pile group (S/D = 3) 59
4.29 Proposed function for p_{mod} (dashed lines) vs FE results (dots) 60
4.30 Proposed function for y_{mod} (dashed lines) vs FE results (dots) 60
4.31 Comparison of p-multiplier with existing method 3-pile group (120°). No gap 61
4.32 Comparison of p-multiplier with existing method 3-pile group (120°). With gap 62
4.33 4-pile group 63
4.34 P-multiplier for 4-pile group (S/D = 2,3,4,5) 63
4.35 fig:y-multiplier 4pile group 64
4.36 Proposed function for p_{mod} (dashed lines) vs FE results (dots) 65
4.37 Proposed function for y_{mod} (dashed lines) vs FE results (dots) 65
4.38 Comparison of p-multiplier with existing method 4-pile group. No gap 66
4.39 Comparison of p-multiplier with existing method 4-pile group. With gap 67

List of Tables

2.1 Ultimate bearing capacity of the wedge failure from literature 10

2.2 P-multipliers from full scale field tests 25

2.3 P-multipliers from model tests 25

2.4 P-multipliers from numerical simulations 25

4.1 Functions for p- and y-multipliers 2-pile group 41

4.2 Functions for p- and y-multipliers 3-pile group (90 ° triangle) 48

4.3 p- and y-multiplier expression for 3-pile group (equilateral triangle) 53

4.4 Functions for p- and y-multipliers for 3-pile group (120 ° triangle) 59

4.5 Functions for p- and y-multipliers 4-pile group 64

5.1 Summary of proposed design expressions for all pile groups 70

Contents

Preface . . . i

Acknowledgment . . . ii

1 Introduction **4**

1.1 Background . . . 4

1.2 Objectives . . . 5

1.3 Limitations . . . 5

1.4 Structure of the Report . . . 6

2 Theory **7**

2.1 Lateral behavior of single piles . . . 8

2.1.1 Failure modes . . . 8

2.1.2 Lateral bearing capacity . . . 9

2.1.3 Modelling the Lateral Response . . . 12

2.2 Lateral behaviour of pile groups . . . 19

2.2.1 Pile Group Interaction Effects . . . 19

2.2.2 Pile Group Effects in Design . . . 21

2.2.3 Industry Practice for Determining p-multipliers . . . 27

3 Parameter Study **28**

3.1 Methodology . . . 28

3.1.1 Finite Element Model . . . 28

3.1.2 Pile Group Configurations and Parameters . . . 30

3.1.3 Material Model . . . 31

3.1.4 Element Mesh . . . 32

3.2 Model Validation . . . 33

3.3 Determining p- and y-multipliers . . . 34

3.3.1 P-multiplier . . . 34

3.3.2 Y-multiplier . . . 34

4 Results **35**
4.1 Validation of Results for Varying stress-strain Response . . . 36
4.2 2-pile group . . . 38
4.2.1 Functions for Determining Group p- and y-multipliers . . . 41
4.2.2 Comparison with existing method . . . 42
4.3 3-pile group (90 ° triangle) . . . 45
4.3.1 Results . . . 45
4.3.2 Functions for Determining Group p- and y-multipliers . . . 48
4.3.3 Comparison with existing method . . . 49
4.4 3-pile group (equilateral triangle) . . . 52
4.4.1 Results . . . 52
4.4.2 Functions for Determining Group p- and y-multipliers . . . 53
4.4.3 Comparison with existing method . . . 53
4.5 3-pile group (120 ° triangle) . . . 57
4.5.1 Results . . . 57
4.5.2 Functions for Determining Group p- and y-multipliers . . . 59
4.5.3 Comparison with existing method . . . 60
4.6 4-pile group . . . 63
4.6.1 Results . . . 63
4.6.2 Functions for Determining Group p- and y-multipliers . . . 64
4.6.3 Comparison with existing method . . . 65

5 Summary and Conclusions **68**

Bibliography **71**

Nomenclature

α	Pile-soil interface roughness
γ'	Effective unit weight of soil
γ^e	Elastic shear strain
γ_f^p	Plastic shear strain at failure
ω	Loading direction
τ	Shear stress
ε_{50}	Strain at 50 % shear stress mobilization in UUTCn an unconsolidated undrained triaxial compression test
D	Pile diameter
E_{py}	Soil pile reaction modulus
E_p	Young's modulus of pile material
I_p	Second moment of inertia of the pile cross section
N_p	Lateral baring capacity factor
N_{pd}	Ultimate lateral bearing capacity factor below transition depth
p_u	Ultimate lateral soil pressure on pile
p_{mod}	p-multiplier
y_{mod}	y-multiplier
G	Shear modulus
J	Empirical factor
p	Lateral soil pressure on pile
s_u	Undrained shear strength of clay
y	Lateral displacement of pile

Chapter 1

Introduction

1.1 Background

Pile groups are commonly used to support offshore jacket platforms. Offshore structures are frequently exposed to significant lateral loading in terms of wind and wave actions. Understanding the lateral pile group response is therefore vital and accurate knowledge of the group effects is required for an optimized design.

The lateral behaviour of pile groups have been studied by several full- and small scale experiments over the years. Based on these tests it has been well established that the average lateral capacity and stiffness of group-pile may be less than a single isolated pile due to soil-pile-soil interaction within the group. However, exact knowledge of the scope of the negative group effects are still limited. The major industry guidelines (DNV, ISO, API) has not updated the references on this subject for many years.

Most of the laterally loaded pile group tests have been performed on array shaped pile groups with normalised center-to-center spacing of S/D = 3. However, the pile groups used for jacket platforms typically consists of only 2 to 4 piles with even closer spacing. The small number of piles makes the group response more susceptible to the loading direction. In field tests it is difficult to distinguish between 'complex' effects like pile driving method and aspect ratio from 'simpler' effects like loading angle and pile spacing. This makes it hard to apply these results to jacket pile groups. Additionally, full scale testing is expensive and technically challenging to conduct. A finite element analysis is a cheaper and more versatile alternative and is well suited for studying the effect of pile spacing and loading direction for different pile group configurations common for jacket platforms. With the current available computational power and advanced soil models a finite element analysis can be performed with sufficient accuracy and is an adequate alternative to real testing.

Problem Formulation

You should define your problem in a clear an unambiguous way and explain why this is a problem, why it is of interest—and to whom. It is also important to delimit the problem area.

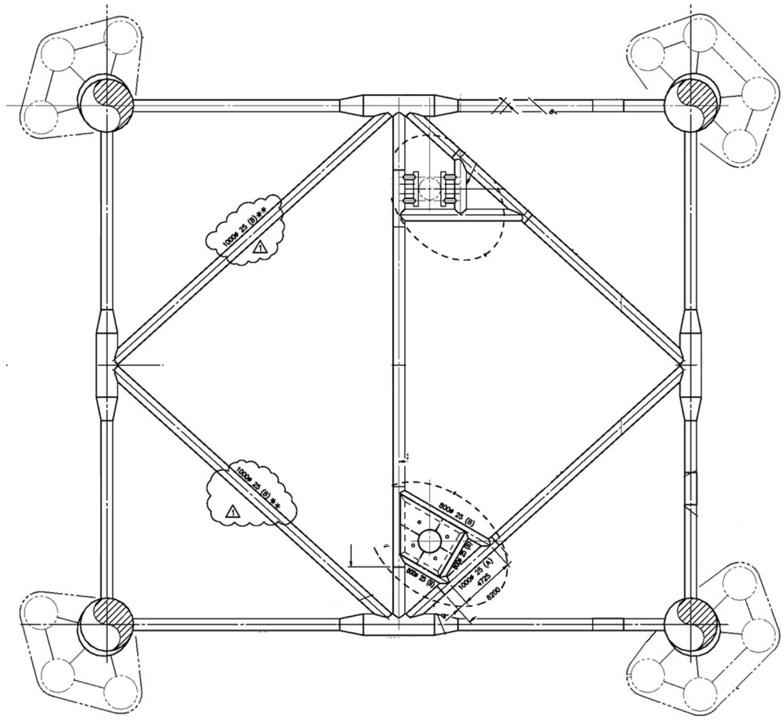

Figure 1.1: Jacket foundation with four legs

1.2 Objectives

The main objectives of this thesis can be listed as the following:

1. Present theory and literature on the subject of lateral bearing capacity of piles and pile groups.
2. Conduct a Finite Element parameter study in ABAQUS to study the effect of pile spacing, loading direction and pile configuration.
3. Establish a set of expressions that can be used predict the p- and y-multipliers for different pile group configurations, pile spacings and loading directions.
4. Compare proposed p- and y-multipliers from the FE study with the currently used design procedure.

1.3 Limitations

Only the plane strain flow-around mechanism of laterally loaded piles is examined in this finite element parameter study. The wedge-type failure is ignored, and the results should only be applied to p-y curves for parts of the pile in the flow-around mechanism.

1.4 Structure of the Report

The rest of the thesis is structured in four main parts. Chapter 2 presents the theoretical background and literature for assessing the lateral response of single piles and pile groups.

In chapter 3 the scope and assumptions of the parameter study is presented.

Chapter 4 presents the results of the parameter study. The results are discussed and expressions to predict p- and y-multipliers are presented. The results are compared to the current industry approach.

Chapter 5 gives a summary and conclusions and presents recommendations for further work.

Chapter 2

Theory

The main purpose of this chapter is to lay out the theoretical background as a basis for the parameter study in Chapter 3. Focus will be on presenting the most widely used design procedure for laterally loaded piles in the industry and the related theory. This includes lateral bearing capacity of piles, modelling the lateral response and negative group effects. The chapter is ended with a comprehensive summary of p-multipliers from the literature, which is directly related to the results of the parameter study. This thesis focus on piles used to support jacket platforms. These piles are long piles with a high L/D ratio and are typically referred to as *slender* piles as opposed to *monopiles*

2.1 Lateral behavior of single piles

2.1.1 Failure modes

Lateral loading of piles will induce two distinct failure mechanisms. At shallow depths the soil will fail in a wedge mechanism. In deeper levels the soil will fail in a localised flow mechanism.

2.1.1.1 Wedge failure

The wedge failure is named after the geometrical shape of the mechanism. A laterally loaded pile will mobilize the soil and a passive and/or active zone with a wedge-like geometry will develop at shallow depths. (Figure 2.1. The suction conditions at the pile will determine whether only a passive zone will develop in front of the pile or if an additional active zone will develop at the rear side of the pile. The suction conditions are related to the presence of soil-pile gaps at the pile. 'Gap' or 'no gap' is refer to a condition of no suction or suction, respectively. If a gap between the soil and the rear side of the pile is present, only only a passive zone will be mobilized in front of the pile. The lateral bearing capacity in this case comes from the mobilized shear strength in the passive zone and the resistance from soil weight. If there is no gap between the pile and soil on the rear side (suction) an additional active zone will develop at the rear side of the pile. In this case the lateral bearing capacity comes from the mobilized shear strength in both the passive and active zone. The bearing capacity from the soil shear resistance is hence doubled, but no resistance from the soil weight is gained because the soil weight from the active and passive soil wedge is equal but acts in opposite directions. The suction conditions at the pile is dependent on several factors. Suction forces may for instance become available due to rapid wave loading or a blocked drainage path caused by a mud mat at the seabed.

The extent of the wedge-type mechanism with depth is limited. The accumulated shear resistance of the wedge failure increase with depth and for a certain depth a local failure mechanism will provide lower lateral resistance and thus become the governing mode of failure. The depth at which the bearing capacity of the wedge failure becomes equal to that of a localised failure is called the transition depth and marks the transition from a wedge mechanism to a flow mechanism.

2.1.1.2 Flow-around failure

Below the transition zone the failure mechanism is no longer influenced by the free soil surface. The soil will fail locally in what is called a flow-around mechanism. The soil "flows" around the pile and no gap between the soil and pile occurs (Figure 2.2). The presence of suction forces implies that the pile behaviour is identical in pulling or pushing in this mechanism. Below the transition zone large overlying soil pressure prevents the soil from moving vertically. A flow-around mechanism can therefore be assumed to take place under plane strain conditions.

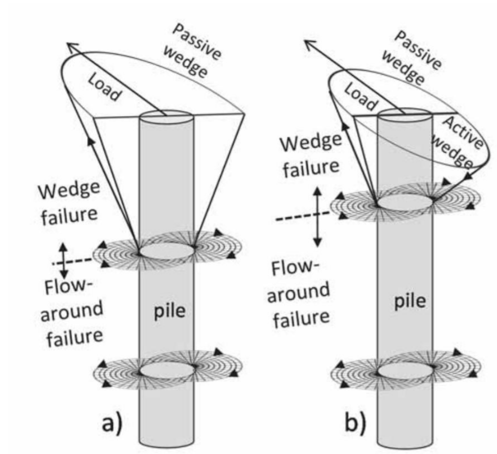

Figure 2.1: Failure modes for a laterally loaded pile (Jeanjean et al. (2017))

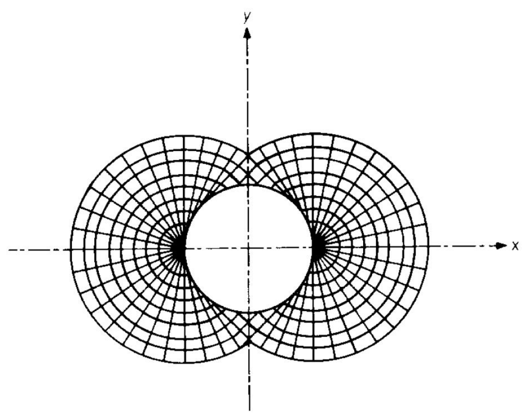

Figure 2.2: Flow around mechanism for a fully rough pile (Randolph and Houlsby (1984)

2.1.2 Lateral bearing capacity

The lateral bearing capacity for a pile in clay can be expressed by the lateral bearing capacity factor:

$$N_p = \frac{p_u}{s_u D} \tag{2.1}$$

where

p_u - ultimate lateral pressure per unit length [kN/m]

s_u - undrained shear strength of clay [kPa]

D - pile diameter [m]

The lateral bearing capacity N_p varies with depth because of different governing failure mechanisms and variation in the resistance they provide with depth. Several researchers have studied the lateral bearing capacity in the wedge for clay. The proposed expressions from different references is presented in Table 2.1

Table 2.1: Ultimate bearing capacity of the wedge failure from literature

Reference	Lateral bearing capacity N_p	Symbol definition
Reese (1957)	$2+\frac{\gamma' z}{s_u}+2\sqrt{2}\frac{z}{D}$	
Matlock (1970)	$3+\frac{Jz}{D}+\frac{\gamma' z}{s_u}$	J is an empirical factor (0.25-0.5)
Murff and Hamilton (1993)	$N_1-N_2 e^{\frac{-\varepsilon z}{D}}$	$N_1=9$ $N_2=7$ $\varepsilon=0.25+0.05\lambda$ for $\lambda<6$ and 0.55 for $\lambda>6$
Nichols et al. (2014)	$4+2(\frac{z}{D})^{0.6*}$	
Jeanjean (2009)	$12-4e^{\frac{-\varepsilon z}{D}}$	$\varepsilon=0.25+0.05\lambda$ for $\lambda<6$ and 0.55 for $\lambda>6$ $\lambda=s_{um}/kD$
Yu et al. (2015)	$N_1-(N_1-N_2)[1-(\frac{z/D}{14.5})^{0.6}]^{1.35}-(1-\alpha)$	$N_1=11.94$ $N_2=3.22$ α= pile roughness

*contribution from soil weight to the bearing capacity is covered by a separate term

The reported expressions for N_p of the wedge failure vary between different references because the wedge mechanism is a fairly complex mechanism and it requires several assumptions to be made. According to Zhang et al. (2016) the most important assumptions contributing to different results for N_p are

- pile-soil roughness
- suction on the rear side of pile
- effect of increasing shear strength with depth
- assumed variation of bearing capacity with depth
- effect of strength anisotropy

Reese (1957) considered a square pile and constant undrained shear strength. Matlock (1970) considered the same pile shape but introduces the empirical factor J calibrated from full scale testings. Murff and Hamilton (1993) performed an upper bound analysis based on plasticity theory for a 3D conical wedge volume. No suction was assumed. Jeanjean (2009) performed centrifuge tests and FEM analyses with suction conditions.Nichols et al. (2014) combined existing literature with complimentary FEM analyses.

A flow-around mechanism can be assumed to take place under plane strain conditions. This makes it a fundamental simpler mechanism to analyze compared to the wedge mechanism. In fact, there exists analytical solutions that are theoretical exact for the lateral bearing capacity, Np, of a pile in flow around conditions. The solutions was given by Randolph and Houlsby (1984). By evaluating the stress field using the method of characteristics Randolph and Houlsby (1984) proposed the following expression for the lateral bearing capacity factor:

$$N_p = \pi + 2\Delta + 2\cos\Delta + 4\left(\cos\frac{\Delta}{2} + \sin\frac{\Delta}{2}\right)$$

Where

$\Delta = sin^{-1}(\alpha)$

α = roughness of the pile.

For the case of a fully rough pile (α = 1) N = $4\sqrt{2} + 2\pi \approx 11.94$. This value is the theoretical exact solution.

Zhang et al. (2016) recommends a revised procedure for determining the lateral bearing capacity with depth. The expression for N_p for the wedge failure is primarily based on Yu et. al. (19xu). Howevr, the revised procedure introduce an additional factor to capture the effect of shear strength heterogeneity. For the flow mechanism the results from Randolph and Houlsby (1984) is adopted with a linear variation from fully smooth ($\alpha = 0$ to fully rough ($\alpha = 1$) pile. The revised procedure for establishing N with depth has since been implemented in the industry guidelines. N_p is given by the following equations:

$$N_{p0} = N_1 - (N_1 - N_2)[1 - \frac{z/D}{d}^{0.6}]^{1.35} - (1-\alpha) \leq N_{pd} \tag{2.2}$$

where

$N_1 = 11.94$

$N_2 = 3.22$

$d = 16.8 - 2.3log(\lambda) \geq 14.5$

$N_{pd} = 9.14 + 2.8\alpha$

Figure 2.3 illustrates the variation of N_p with depth as given by Equation 2.2. N_p is calculated for two different soil profiles and pile diameters. A fully rough pile-soil interface and gapping conditions are assumed. The latter imply contribution to the resistance from soil weight, with a unit weight of $\gamma' = 7kN/m^3$ and $\gamma' = 10kN/m^3$ for the lightly over-consolidated and highly over consolidated soil profile, respectively. N_p = 3.22 at the surface level and is gradually increasing until the transition depth is reached where N_p = 11.94. At this depth the flow-around failure is governing and N_p is constant with depth. It becomes evident that both the pile diameter and the soil strength heterogeneity affect N_p and the onset of a localised flow around failure mechanism.

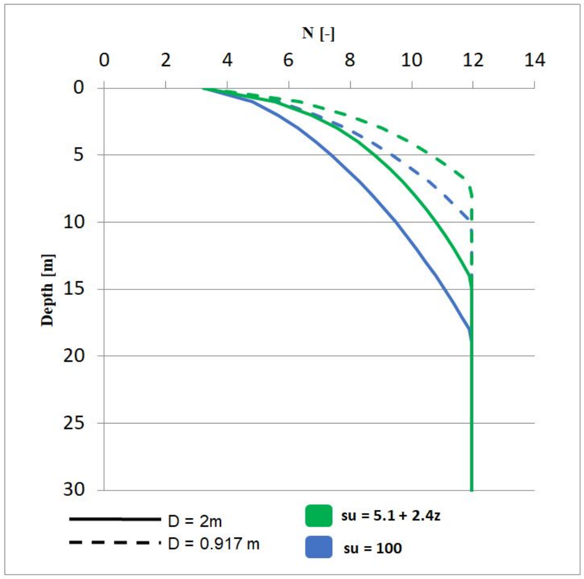

Figure 2.3: Variation of N_p with depth for two soil profiles and pile diameters

2.1.3 Modelling the Lateral Response

Loading of piles is a classic soil-structure interaction issue where the behaviour of both the soil and pile is mutually dependent components. The combined response of axially and horizontally loaded piles is analyzed by a beam-column analysis. More specifically, a beam on non-linear foundation, also known as a non-linear Winkler foundation, is used to model the lateral response.

2.1.3.1 Winkler foundation

The concept of a beam on elastic foundation (BEF) was first introduced by Winkler (1867). The main premise of Winkler's formulation is a beam subjected to a distributed reaction force (q) that is proportional to the foundation displacement (z) (Figure 2.4).

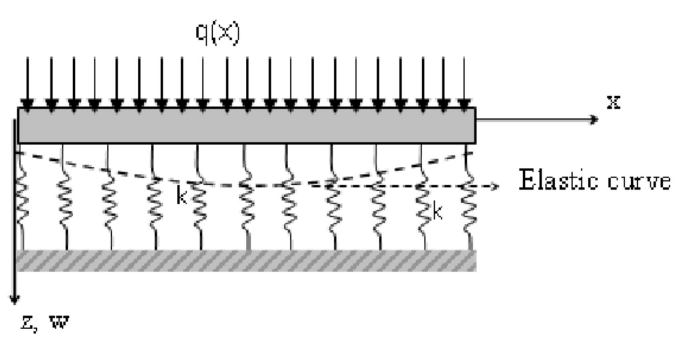

Figure 2.4: Principle of a Winkler foundation (Karasin and Aktas (2014)

In structural terms the relationship between the reaction force (q) and the foundation displacement (z) is modelled as springs. In geotechnics and the subject of laterally loaded piles the pile displacement and soil resistance relationship is approximated by springs referred to as p-y springs, p-y curves or more generally load transfer curves. As demonstrated in section 2.1.2 the lateral bearing capacity vary with depth. Consequently it is necessary to apply different springs along the pile in order to accurately model the lateral soil response. In practice the pile is discretized in finite sections. Each section has a corresponding p-y spring that govern the lateral soil resistance for that particular part of the pile (Figure 2.5).

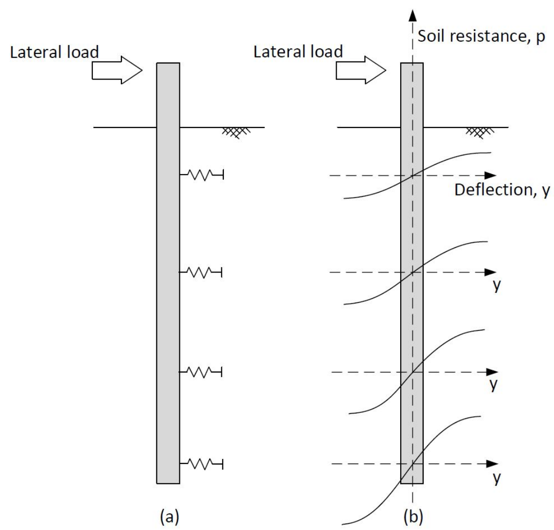

Figure 2.5: Modelling of the lateral pile response with p-y springs (Fayyazi (2015)

An important implication of the discretization process is that the soil resistance (p) wil only be dependent on the displacement (y) of the particular discretized section. That is, each spring operates independently of each other. The Winkler approach is therefore unable to represent the true continuous behaviour of the pile-soil system. However, this simplification does not provide substantial errors Kagawa (1992). The accuracy of the results are directly and predominantly dependent on how well the springs can describe the in-situ soil behavior. Focus should consequently be put on developing satisfactory soil springs for that can accurately describe current soil and pile conditions.

2.1.3.2 Governing Differential Equation

The pile-soil interaction problem requires solving a 4th order differential equation of a beam on non-linear foundation derived by Hetenyi (1946).

$$E_p I_p \frac{d^4 y}{d^4 x} + P_x \frac{d^2 y}{d^2 x} + E_{py} y = 0 \tag{2.3}$$

where

y - Lateral displacement

x - Point along the pile

E_p - Young's modulus of the pile material

I_p - Second moment of inertia of the pile cross section

P_x - Vertical load

E_{py} - Soil reaction modulus

It is important to note that E_{py} is not the classic Young's modulus of soil. Instead, E_{py} describes the relation between the soil resistance and pile displacement. This relation is not uniquely a soil property, but is also dependent on the pile geometry. Sometimes E_{py} is referred to as the 'modulus of subgrade reaction' in the literature. The 'modulus of subgrade reaction' was initially introduced as a concept to relate foundation pressure to foundation settlements and engineers should therefore be cautious of not mixing the two measures.

A constant value for E_{py} along the entire pile was utilized in the earliest analyses of laterally loaded piles. A constant value of E_{py} implies a linear relationship between the soil displacement and the reaction force. This simplification made it possible to develop analytical solutions of the differential equation (Equation 2.3) for different boundary conditions. However, using the same value for E_{py} for the entire depth is not good idealization of the real soil behavior. Furthermore, soil is well known to show a highly non-linear stress-strain relationship. Based on these acknowledgements, McClelland and Focth (1956) introduced the concept of non-linear p-y curves. The p-y curves enabled engineers to describe an arbitrary variation of E_{py} both with respect to depth and pile displacement. E_{py} is accordingly a function of both x and y and the equation Equation 2.3 cannot be solved analytically. An appropriate numerical method, most commonly a finite difference scheme, can be employed. Using a numerical method poses poses no limitations to the method following great advancement in available computational power over the years. The system of equations can typically be solved by a desktop computer in a matter of seconds. A time efficient method is a great advantage, especially in off-shore structural design, where the number of load cases can be several thousands. (Muskulus and Schafhirt (2014)).
Figure 2.6 shows the relationship between the different load effects that are obtained by solving the differential equation. These measures are of crucial interest in design.

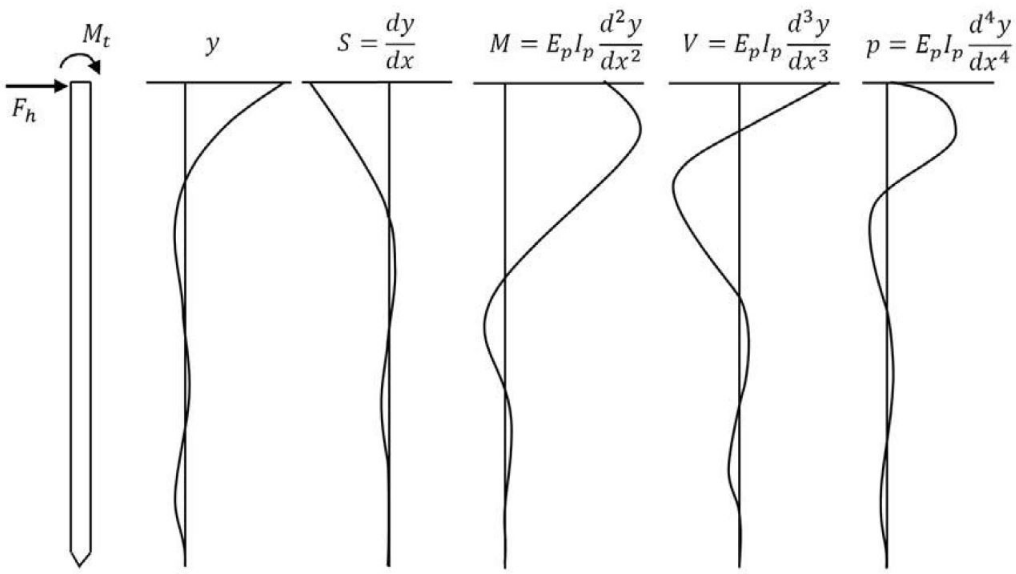

Figure 2.6: Relationship between the displacement, slope, bending moment, shear force and soil pressure of the pile (Reese and van Impe (2010)

2.1.3.3 P-y Curves

Figure 2.7 illustrates a p-y curve with the characteristic non-linear shape. For a given level of mobilization, the soil resistance (p) is related to the lateral pile displacement (y) by the soil reaction modulus E_{py}. Important features of a p-y curve is the initial stiffness $E_{py,max}$, the ultimate capacity p_u and the reduction of E_{py} with displacement. The latter property defines the curve shape and thus the stiffness of the pile-soil system. The ultimate capacity of a p-y is governed by the lateral bearing capacity related to the different failure mechanism as discussed in section 2.1.2 while the shape of the curve is mainly dependent on soil stress-strain characteristics, which can be obtained from laboratory tests.

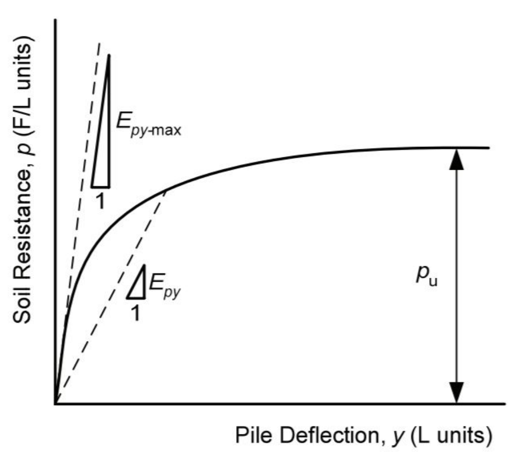

Figure 2.7: A general p-y curve (Dodds and Martin (2007))

P-y curves provide a practical method for modelling the lateral soil resistance, but procedures for accurately constructing the curves are vital in order to achieve accurate and reliable results for design. Research on the topic of p-y curves was initiated by the needs of the offshore petroleum industry emerging in the middle of the last century. The first major study on the topic was done by McClelland and Focth (1956). McClelland and Focth (1956) performed full-scale testing of piles in the Gulf of Mexico. Closely spaced strain gauges were applied along the pile surface. Bending moments can then be calculated using the moment curvature relation. A complete moment distribution is obtained by curve fitting the acquired moment values. This enabled the pile displacement (y) and the soil resistance (p) to be determined for several load increments by utilizing the relations in Figure 2.6. The next is to calibrate the experimentally obtained p-y curves with $\tau - \varepsilon$ soil behaviour from laboratory testing. Because of limited data McClelland and Focth (1956) did not manage to develop a comprehensive method for constructing p-y curves, but their experiments has inspired future work on the subject. (Reese and van Impe (2010))

Following McClelland and Focth (1956), the perhaps most widely recognized research on the topic of p-y curves is the work done by Matlock (1970), Reese et al. (1975) and O'Neill and Murchison (1983). which have proposed procedures for constructing p-y curves in soft clay, stiff clay and sand, respectively. Despite that these references are several decades old they are still referred to as the recommended methods in major industry standards like API (2014), ISO (2014) and DNV (2017).

2.1.3.4 P-y Curves for Clay

The most relevant p-y curves for offshore pile groups are soft clay ($s_u < 100kPa$). Matlock (1970) performed field and laboratory testing of soft clay from Lake Austin and the Sabine river. He utilized the same experimental techniques for obtaining p-y curves as McClelland and Focth (1956). Matlock (1970) proposed a limiting capacity for the p-y of

$$N_p = 3 + \frac{Jz}{D} + \frac{\gamma' z}{s_u}$$

and limited by

$$N_p = 9$$

for the flow around mechanism.

The soil $\tau - \varepsilon$ properties from laboratory tests is related to the experimentally obtained p-y curves using a power function on the form:

$$\frac{p}{p_u} = 0.5\left(\frac{y}{y_{50}}\right)^{1/3}$$

where

$y_{50} = 2.5\varepsilon_{50}$D

D = pile diameter

ε_{50} = value of strain where 50 % of the maximum shear stress has been mobilized in an unconsolidated undrained triaxial compression test.

Some more recent work on the topic of p-y curves in clay include, among others, Jeanjean (2009) and Zhang and Andersen (2017). Based on centrifuge tests and finite element analyses Jeanjean (2009) proposed the following relation for constructing p-y curves in clay:

$$\frac{p}{p_u} = \tanh\left(\frac{G_{max}}{100 s_u}\left(\frac{y}{D}\right)^{0.5}\right)$$

Zhang and Andersen (2017) obtained an extensive amount of p-y curves by performing a finite element parameter study of a pile slice in PLAXIS for a wide range of soil stress-strain relations and pile roughness interface values. A method for scaling the soil stress - strain relationship of the soil to p-y curves was developed. The p-y curve is constructed by scaling the plastic and elastic shear strain components to the normalised displacement (y/D), such that p/p_u = τ/s_u. A scaling coefficient ζ_1 = 2.8 and ζ_2 = 1.35+0.25α is applied to the elastic and plastic shear strain components, respectively. The concept is illustrated in Figure 2.8

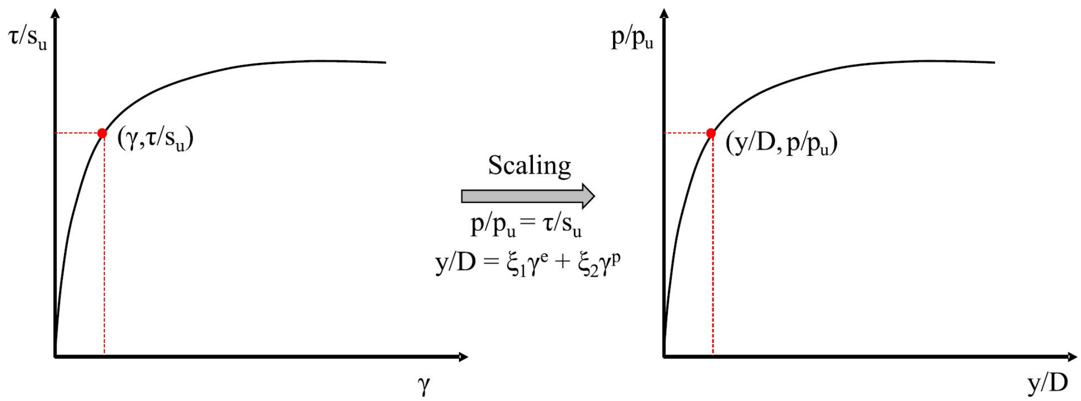

Figure 2.8: Concept of scaling soil stress-strain curve to a p-y curve (Zhang and Andersen (2017))

2.2 Lateral behaviour of pile groups

In practice piles are almost always used in groups of two or more piles in order to increase the total bearing capacity. The capacity of a pile group is the sum of the capacity from each individual pile in the group. However, because of pile-soil-pile interaction effects, the ultimate lateral bearing capacity and the stiffness of a group-pile may be less than an equivalent isolated single pile.

2.2.1 Pile Group Interaction Effects

Pile group interaction effects can be explained by interacting stress zones in the soil. When no external lateral load is applied an uniform soil pressure is acting on the pile (Figure 2.9a). When an external lateral load is applied the pile experience an increased lateral soil pressure (Figure 2.9b). The zones of mobilized soil is often referred to as shear zones. In the case of a pile group, two or more piles are in close proximity to each other. This may cause the shear zone of one pile to overlap the shear zone of adjacent pile(s). Overlapping of shear zones reduces the available resistance of the soil and results in loss of ultimate bearing capacity and stiffness. Overlapping of shear zones from the same row is commonly refereed to as 'shadowing effects' while overlapping of shear zones from piles in the same row is called 'edge effect'. (Walsh (2005)). The respective interaction effects are illustrated on Figure 2.10.

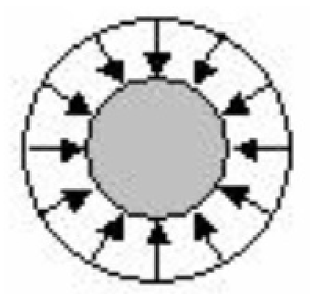

(a) Uniform soil pressure

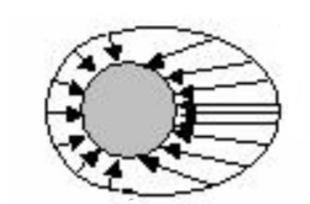

(b) Non-uniform soil pressure

Figure 2.9: Lateral soil pressure on pile for different loading conditions (Pando et al. (2006))

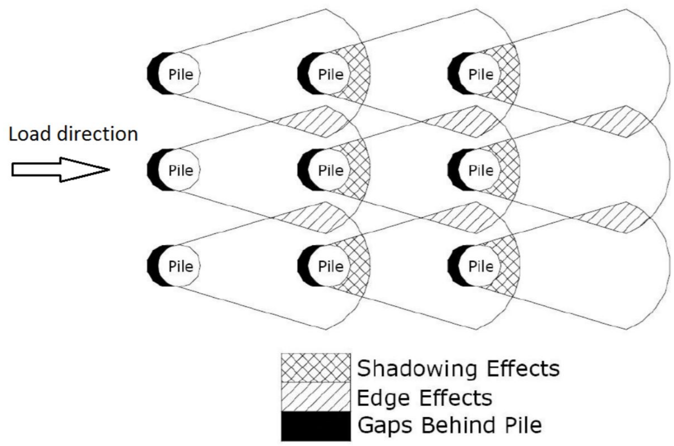

Figure 2.10: Shadow and edge effects in pile groups (Walsh (2005)

Much of the early understanding of pile group interaction effects from pile group testing, particularly in the 1980s. Meimon and Jezequel (1986) showed that group interaction effects were negligible for small pile displacements. For small displacements the piles behave as single isolated piles because the soil is not mobilized enough for shear zone overlapping to occur. Meimon and Jezequel (1986) also showed that the leading pile rows experienced higher bearing bearing capacity than trailing pile rows, i.e the effect of shadowing effect is stronger for trailing piles. The latter effect is also also been in several other pile group experiments. Figure Figure 2.11 shows a load-deflection curve from pile group testing done by Rollins et al. (2006) and illustrates the loss of ultimate bearing capacity and stiffness due to group interaction effects..

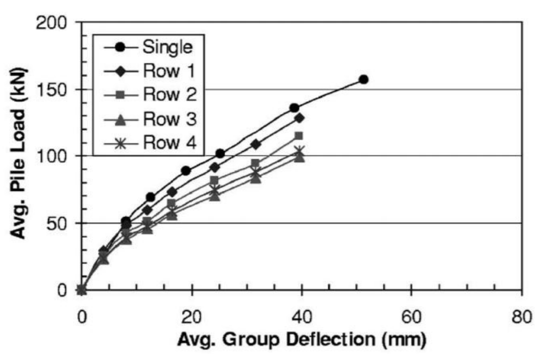

Figure 2.11: Pile group test load - deflection curve (Rollins et al. (2006))

The reason many piles tests show an increasingly stronger shadowing effect for trailing piles is related to the suction conditions during the test. When no suction is present in the upper parts of the pile a gap will form and only soil in front of the pile is mobilized. The shear zones from leading piles will overlap the shear zones from trailing piles, but not vice versa. On the contrary, if there is suction available an equal amount of soil will be mobilized both in front and behind the pile. In that case a leading and trailing pile will experience the same reduction of bearing capacity caused by mutual overlapping of the shear zones. That is, when suction forces are present there is no difference between pushing or pulling the pile group or between the response of leading or trailing piles.

2.2.2 Pile Group Effects in Design

According to the industry standards API (2014), ISO (2014) and DNV (2017) group interaction effects shall be considered if the pile center-to-center spacing is less than 8 pile diameters. Some conditions that may influence the pile group response are mentioned:

- Pile spacing
- Pile penetration to diameter
- Pile soil-relative stiffness
- Pile installation method
- Soil layering

The standards refer to several publications, mainly from the 1970s and 80s, to account for group effects in design. The earliest references are based on theory of elasticity. Poulos and Davis (1980) assumed the soil to be an elastic continuum and proposed interaction factors to account for a reduced stiffness of the pile group. The interaction factors give the total pile displacement as a superposition of the local displacement of a pile and displacement due to interaction from adjacent pile(s) as a function of the pile spacing and loading angle.

Focht Jr and Koch (1973) proposed a hybrid method by combining the elastic interaction factor approach from Poulos and Davis (1980) with the non-linear p-y spring approach. In this method the local displacement of the piles are modelled using traditional p-y curves while elastic interaction factors are used to predict displacements due to group interaction. When the total group deflections are known, each single pile p-y curve can be modified by multiplication of a y-multiplier to match the group displacement. The y-multiplier is a factor with a numerical value > 1 that is applied to the displacement (y) axis of the p-y curve. A y-multiplier will stretch the p-y curve resulting in a greater magnitude of displacement for the same mobilization of soil pressure (Figure 2.12).

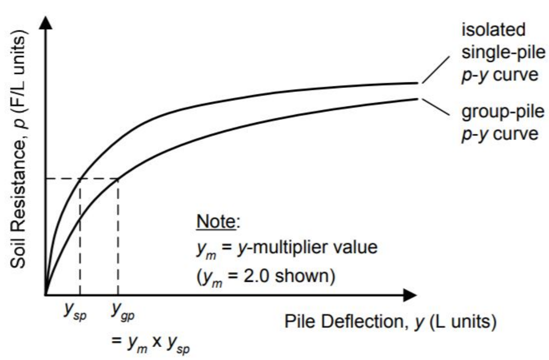

Figure 2.12: Concept of the y-multiplier (Dodds and Martin (2007))

Bogard and Matlock (1983) proposed a closed form method for obtaining group p-y curves based on a key concept for laterally loaded pile groups:

1. Some portion of displacement is due to local deformation around individual piles within the group.

2. Some portion of displacement is is due to displacement of soil mass surrounding the pile group as a whole

A p-y curve for the local displacement (1) can be constructed by treating the pile as a single pile (no group effects). A p-y curve accounting for the second part (2) is treated by constructing a p-y curve for an imaginary pile with a diameter equivalent to the area enclosing the pile group. The p values of the second p-y curve is obtained by dividing by the number of piles and y values are obtained by dividing with the center spacing of the pile. The displacement of the two p-y curves, representing effect (1) and (2), is superposed as illustrated in Figure 2.13

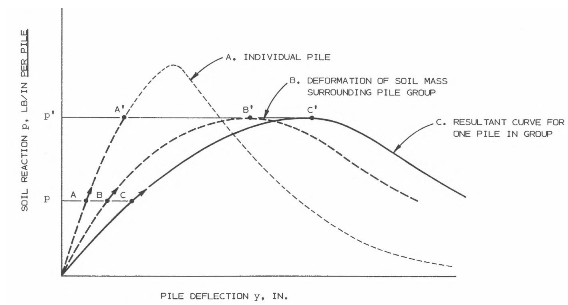

Figure 2.13: Bogard and Matlock's concept for generating group-pile p-y curves (Bogard and Matlock (1983))

Pile group response is calculated using a Winker approach with nonlinear p-y springs similar to that of single piles. The lateral bearing capacity of a pile group consisting of N piles are calculated as either:

1. N times the capacity of a single pile with modified p-y curve or
2. The capacity of an equivalent imaginary pile with a diameter equivalent to the area enclosing the piles

Modification of the p-y curves can be done using the above closed form or elasticity theory based references from the standards.
As an addition to the elasticity based methods using y-multipliers, the industry guidelines also allows for the use of p-multipliers. The concept of p-multipliers was introduced by Brown et al. (1988). It resembles the results from Bogard and Matlock (1983), in which a p-y curve for a group-pile is obtained by reducing the magnitude of soil pressure (p) that is mobilized at a given displacement (y). However, using p-multipliers are easier compared to the method of Bogard and Matlock (1983). The p-multiplier is simply a reduction factor with a numerical value < 1 that is applied to p-axis of a the p-y curve. The p-y curve will be "flattened" with reduced ultimate capacity and stiffness in accordance to the group effects. The concept is illustrated in Figure 2.14 .

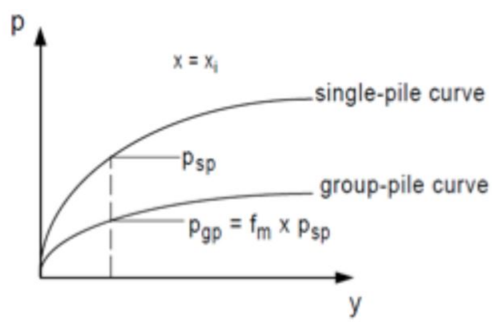

Figure 2.14: Concept of the p-multiplier (Dodds and Martin (2007)

In principle a distinct p-multiplier should be applied to every row or pile based on interaction effects. As an alternative to differentiate between different piles or rows, Brown et al. (2001) proposed a group p-multiplier. In this case the same group p-multiplier is applied to all piles in the group irrespective of row or pile location. The group p-multiplier is simply the average of the p-multipliers for the different piles. The obvious advantage of using a group average p-multiplier is that it makes for a simplified design approach. It is especially useful in situations where the loading direction constantly changes, i.e for cyclic loading. Brown et al. (2001). P-multipliers have been studied by many researchers over the years using different experimental methods that can be categorized as

- Full scale field tests
- Model tests
- Numerical simulations

Full scale tests are performed in the field with real soil and piles. A full size test has the obvious advantage of being able to capture the actual in-situ behaviour. On the down side full-scale tests are technically challenging

and expensive to perform. (Fayyazi (2015)). Due to limiting capacity of the loading equipment full scale tests are generally performed on no larger than 3x3 pile groups with low spacing ratios (S/D <= 3).
Model tests are a cheaper alternative to full scale testing. Model tests include 1g testing and centrifuge testing in the laboratory.
Numerical analyses is a versatile and cost-effective method. The method primarily includes the use of the finite element method or other continuum methods to model the pile-soil-pile interaction effects. With an ever increasing advancement in available computational power and the development of realistic material models, numerical simulations can be an accurate and reliable tool for analyzing a wide range of geotechinical problems, including lateral pile group effects.

Table 2.2, Table 2.3 and Table 2.4 summarize reported p-multipliers from different references for full scale field tests, model tests and numerical simulations, respectively. P-multipliers by row for 3x3 pile groups and S/D from field and model tests in clay and sand is illustrated in Figure 2.15. Based on these data some general remarks can be made:

- There is an apparent scatter in reported p-multipliers between different references, even for the same pile configurations and spacing ratios
- the group effects can be very significant, with reported loss of efficiency surpassing 50 %
- p-multiplier decrease with increasing row number in the direction of loading
- p-multiplier decrease with increasing pile group size
- p-multiplier increase with increasing normalized spacing ratio.
- There is not enough available data to make a certain distinction between the p-multiplier in clay and sand across different experiments.

Table 2.2: P-multipliers from full scale field tests

Row number									
Reference	Soil type	Pile configuration	S/D BC	1	2	3	4	5	Group average
Meimon and Jezequel (1986)	Clay	3x2	3	0.90	0.50	0.70	-	-	0.70
Brown and O'Neill (1987)	Clay	3x3	3	0.70	0.60	0.50	-	-	0.60
	Clay	3x3	3	0.70	0.50	0.40	-	-	0.53
Brown et al. (1988)	Sand	3x3	3	0.80	0.40	0.30	-	-	0.50
	Sand	3x3	3	0.80	0.40	0.30	-	-	0.50
Morrison and Reese (1988)	Sand	3x3	3	0.80	0.40	0.30	-	-	0.50
	Sand	3x3	3	0.80	0.40	0.30	-	-	0.50
Ruesta and Townsend (1997)	Sand	4x4	3	0.80	0.70	0.30	0.30	-	0.53
Rollins et al. (1998)	Clay	3x3	3	0.60	0.38	0.43	-	-	0.47
Huang et al. (2001)	Clay	2x3	3	0.93	0.70	0.74	-	-	0.79
	Clay	3x4	3	0.89	0.61	0.61	-	-	0.69
Rollins and Sparks (2002)	Clay	3x3	3	0.60	0.38	0.43	-	-	0.47
Snyder (2004)	Clay	3x5	4	1.00	0.81	0.59	0.71	0.59	0.74
Walsh (2005)	Sand	3x5	4	1.00	0.50	0.35	0.30	0.4	0.51
Rollins et al. (2005)	Sand	3x3	3	0.80	0.40	0.40	-	-	0.53
Christensen (2006)	Sand	3x3	3	1.00	0.7	0.65	-	-	0.78
Rollins et al. (2006)	Clay	3x5	3	0.82	0.61	0.45	-	-	0.62

Table 2.3: P-multipliers from model tests

Row number									
Reference	Soil type	Pile configuration	S/D	1	2	3	4	5	Group average
McVay et al. (1995)	Loose sand	3x3	5	1.00	0.85	0.70	-	-	0.85
	Dense sand	3x3	5	1.00	0.85	0.70	-	-	0.85
	Loose sand	3x3	3	0.65	0.45	0.35	-	-	0.48
	Dense sand	3x3	3	0.80	0.40	0.30	-	-	0.50
McVay et al. (1998)	Sand	3x3	3	0.80	0.40	0.30	-	-	0.50
	Sand	3x4	3	0.80	0.40	0.30	0.30	-	0.45
	Sand	3x5	3	0.80	0.40	0.30	0.20	0.30	0.40
Ilyas et al. (2004)	Clay	2x1	3	0.80	0.63	-	-	-	0.72
	Clay	2x2	3	0.86	0.78	-	-	-	0.87
	Clay	3x3	3	0.65	0.50	0.48	-	-	0.54
	Clay	4x4	3	0.65	0.49	0.42	0.46	-	0.51
Chandrasekaran et al. (2010)	Clay	2x2	3	0.74	0.48	-	-	-	0.61
	Clay	2x2	5	0.85	0.58	-	-	-	0.87
	Clay	3x3	3	0.66	0.41	0.44	-	-	0.50
	Clay	1x4	3	0.76	0.56	0.46	0.54	-	0.58

Table 2.4: P-multipliers from numerical simulations

Row number									
Reference	Material model	Pile configuration	S/D	1	2	3	4	5	Group average
Budiman and Ahn (2005)	Cam clay	1x3	3	1.59	0.75	0.77	-	-	-
Al-Jubair and Abbas (2014)	MC	3x1	3	1	0.68	0.68	-	-	0.79
	MC	2x2	3	0.82	53	-	-	-	0.68
Fayyazi et al. (2014)	MC	3x3	3	-	-	-	-	-	0.55
Allahverdizadeh (2015)	MC	3x3	3	0.78	0.40	038	-	-	0.52
Abbas Al-Shamary et al. (2018)	MC	2x1	3	0.56	0.43	038	-	-	0.50
	MC	3x2	3	0.5	0.39	0.26	-	-	0.38
Alkloub et al. (2018)	MC	2x2	3	-	-	-	-	-	0.67
	MC	3x1	3	-	-	-	-	-	0.74

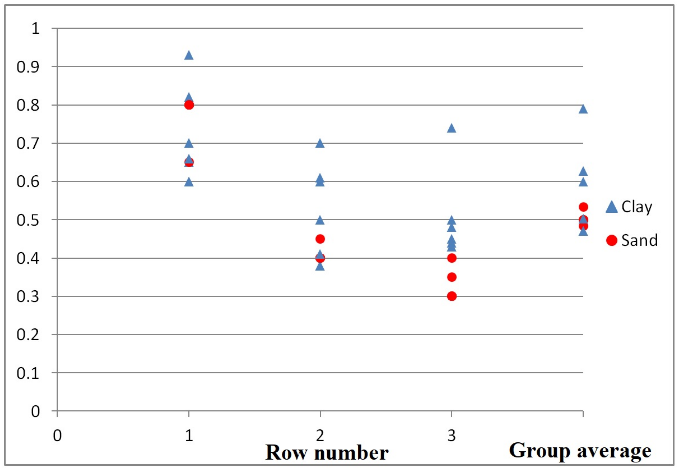

Figure 2.15: P-multiplier from model and full scale tests for 3x3 pile groups (S/D = 3) in clay and sand

A p-multiplier will incorporate several factors in a single measure. This presents challenges when studying p-multipliers from field tests as it becomes difficult to distinguish 'complex' effects from 'simpler' effects. Complex effects may for instance be the type of pile driving method used to install the piles. Huang et. al. (2001) and Brown et. al. (2001) both reported a difference in the obtained p-y curves from field tests of driven and bored piles of up to 40 %. Another 'complex' factor may be the aspect ratio, that is the penetration depth over the pile diameter (L/D) and the relative stiffness of the pile and soil. Sazzad et al. (2019) reported that the aspect ratio had a significant impact on the load-deflection characteristics of the pile. This may impact the results because the group effect is dependent on the degree of soil mobilization which in turn is directly dependent on the displacement of the piles in the soil. 'Complex' effects are a contributing factor to why the p-multipliers vary between different experiments. 'Simpler' effects are referred to parameters that are more straightforward to study, like the effect of pile spacing (S/D) and loading direction angle.

Another important aspect of the p-multiplier is the variation with depth. The reported p-multipliers in Table 2.2 are based on back calculations. One way of determining the p-multiplier is to back calculate the overall response of the pile group. That is, the p-multiplier value for a given pile, row or group is altered in the back calculation (i.e. using a computer program) until the calculated response matches the overall measured response from experiments. A common response criteria is to require equal pile head deflections for a given load in the back calculation and experiment. In this approach the p-multiplier is constant with depth. A constant p-multiplier with depth is sufficient as long as the overall back calculated group response align with the experimental results.
Alternatively, if the piles are installed with suitable equipment (i.e. strain gauges) to re-create local p-y curves with depth, the p-multiplier can be determined by back-fitting the local p-y curve data.
The latter approach was utilized by Brown et al. (1988). The results showed no apparent trend of the p-multiplier with depth for $z/D < 2$. It was not possible to re-create p-y curves for $z/D > 2$ because of limited pile displacements because the largest lateral deflections occurs near the surface and are governing the lateral behavior.

2.2.3 Industry Practice for Determining p-multipliers

NGI currently use a method for determining p-multipliers that compares the sum of the local bearing capacity of each pile in the group to the capacity of an equivalent pier (Figure 2.16). The procedure is as follows:

1. Calculate the diameter of a pile with same area as an equivalent pier.
2. Calculate the lateral capacity of the pile from Step 1: $p_{u,1} = N_1 \cdot s_u \cdot D_1$
3. Calculate the sum of lateral capacity of n-piles group. $p_{u,2} = n \cdot N_2 \cdot s_u \cdot D_2$
4. The group efficiency (p-multiplier) is determined by dividing the acquired capacity from step 2) by the capacity from step 3. p-mod = p_1 / p_2

Example: if the capacity of the larger equivalent pile at a given depth z is $p_{u,1}$ = kN/m and the capacity of the sum of each pile in the gorup is $p_{u,2}$ = 300 kN/m, the p-multiplier becomes 200/300 = 0.67. This implies a loss in bearing capacity due to interaction effects. Alternatively, if the capacity of the larger imaginary pile is $p_{u,1}$ = 300 and the sum of each indvidual pile is $p_{u,2}$ = 200, the p-multiplier is 1. This implies no loss or bearing capacity and the piles are assumed to fail locally without interacting.

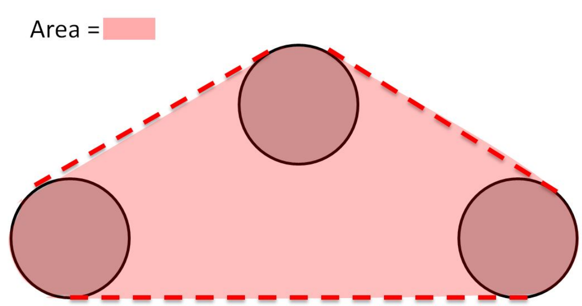

Figure 2.16: An equivalent pier defined from a 3-pile group

Chapter 3

Case Study of Lateral Group Effects

This chapter presents the methodology of the case study of pile group interaction effects. The study of group effects are based on numerical simulations in the commercially available finite element software ABAQUS 2017.

3.1 Methodology

3.1.1 Finite Element Model

The finite element model is illustrated in Figure 3.1. The model represents a horizontal slice of the pile group and surrounding soil. The slice has a unit thickness of 1m. The model is appropriate for simulating a localised flow-around failure mechanism. The top and bottom boundaries of the model are constrained for vertical displacement in order to enforce plane strain conditions. The piles are modelled as rigid body objects. Additionally the piles are constrained against torsional rotation. The piles have a diameter of 2m and are located in the center of the model. The distance from the pile edges to the model boundaries are at least 10D. This ensures sufficient distance from the model edges to ensure that boundary effects do not significantly influence the pile group behavior.

The analysis is performed using displacement control. A lateral displacement is applied to the center of each pile causing the pile slices to translate as rigid bodies in the soil. The total magnitude of soil pressure (p) acting on each pile for a given magnitude of displacement (y) is measured in ABAQUS and p-y curves can be obtained as a direct output from the analysis results. To make sure that the ultimate capacity is reached, displacement of the piles are prolonged until the p-y curve does not show a significant increase in pressure with increasing displacement. The pile-soil interface is set to fully rough (α=1) in the analyses.

It is important to emphasise that only a local flow-around mechanism is modelled in the present analysis. The wedge failure mechanism is consequently ignored for this study. Results from this study are therefore in principle only valid for parts of the pile below the transition depth X_R, where a localised flow-around mechanism is the governing mode of failure.

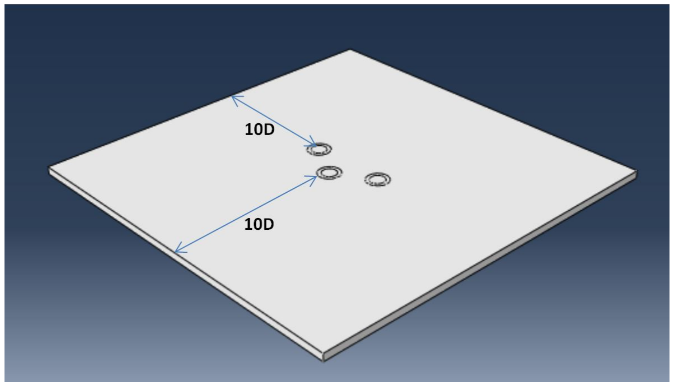

Figure 3.1: Finite element model of a 1 m soil and pile group slice

3.1.2 Pile Group Configurations and Parameters

The studied pile group configurations are presented in Figure 3.2. The pile group configurations includes a 2-pile group, a 4-pile square pile group and three 3-pile pile groups. The loading direction ω is counter clockwise relative to the horizontal line ($\omega = 0°$) and related to the current group orientation in Figure 3.2. Each pile group configuration is analyzed for a normalised center-to-center ratio of S/D = 2,3, 4 and 5. The corresponding S/D ratio for the different pile groups are as illustrated in Figure 3.2.

The symmetry line(s) of the pile groups are illustrated by dashed lines in Figure 3.2. The symmetry line(s) represents a loading direction that give an identical response, while the response will vary in the range spanning the line(s) of symmetry. Each pile group is therefore analyzed for multiple angles that span the line(s) of symmetry in order to capture the entire pile group response.

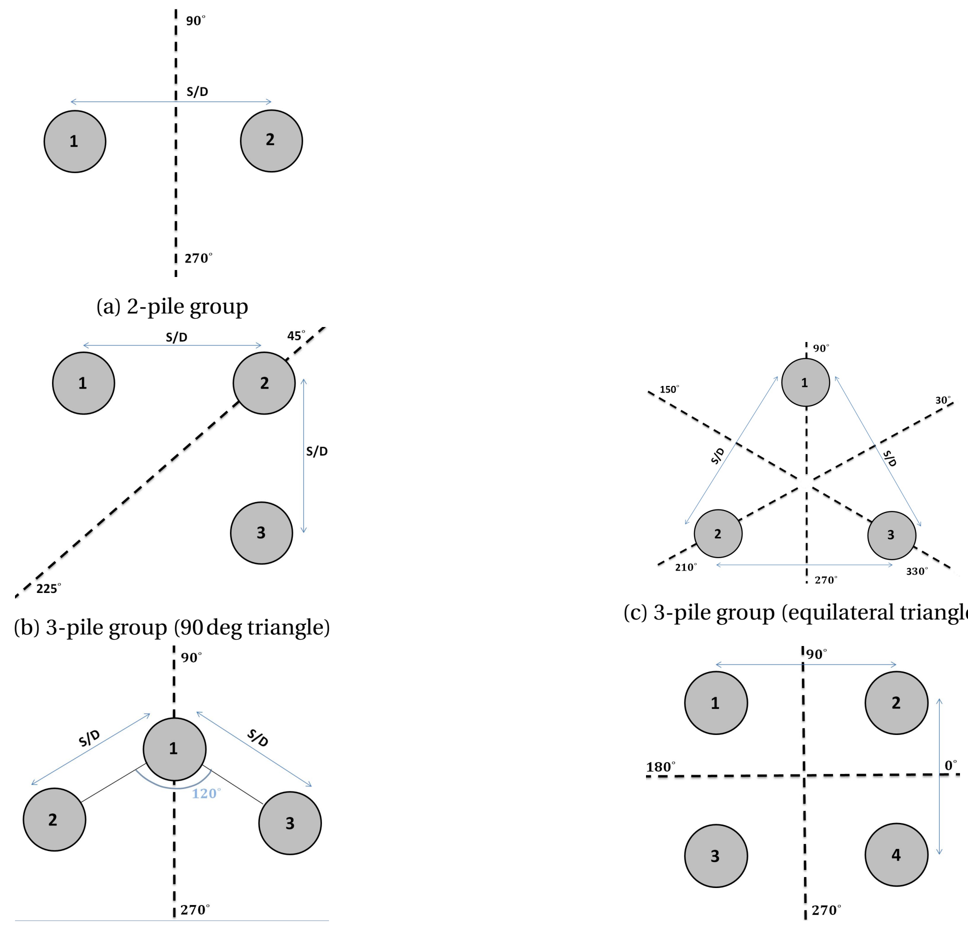

(a) 2-pile group

(b) 3-pile group (90 deg triangle)

(c) 3-pile group (equilateral triangle)

(d) 3-pile group (120 deg triangle)

(e) 4-pile group (square)

Figure 3.2: Analyzed pile group configurations

3.1.3 Material Model

For the present study clay is considered. The NGI-ADP model (Grimstad et al. (2012)) is used to describe the clay stress-strain response. The NGI-ADP material model gives the desired non-linear stress-strain relationship of the soil. The non-linear stress-strain relationship is described by the following normalized strain hardening curve:

$$\kappa = 2\frac{\sqrt{\gamma_p/\gamma_p}}{1+\gamma_p/\gamma_{pf}}$$

Where

κ = Mobilized shear stress (τ/s_u)

γ_p = current plastic shear strain

γ_{pf} = plastic shear strain at failure

In the NGI-ADP model the above strain hardening curve is used to describe both the active, passive and direct shear conditions in the soil. However, the plane strain flow mechanism in this study can assumed to be governed a direct shear mode only. Interpolation between the active, passive and shear mode is thus not necessary and the strain hardening curve from the NGI-ADP model can be implemented directly in ABAQUS using 'Mohr-Coulomb Plasticity' by specifying the plastic shear strains γ^p for different levels of shear stress mobilization. The elastic shear component γ^e is governed by the elastic parameters ν and G_{max}/s_u. The total shear strain at a given level of mobilized shear stress is the sum of the plastic and elastic shear strains.

Material parameters chosen for the analyses is $s_u = s_u^{DSS}$ = 100 kPa, γ_{pf} = 5% and G_{max}/s_u = 500. Some additional analyses are performed with γ_{pf} = 10% and γ_{pf} = 15% for certain parameter cases in order to verify the generality of the results for a wider soil stress-strain range.

3.1.4 Element Mesh

The element mesh consists of C3D8R elements. This is a linear solid brick element with one integration point located in the center of the element. Because of the location of the integration point within the element a lot of elements of this type is required where high stress concentrations occur (i.e. pile-soil boundary), as the stresses are most accurately estimated in integration point. However, due to the low order of the C8D8R element sufficiently many elements can be generated for this model without enforcing too high computational cost. Figure 3.3 illustrates a representative element mesh used in this study. The mesh is very refined in an area of radius 1D around the piles and the mesh gets coarser towards the model boundaries. The total number of elements used to generate the models in this study vary between 40.000-50.000 depending on pile configuration and pile spacing.

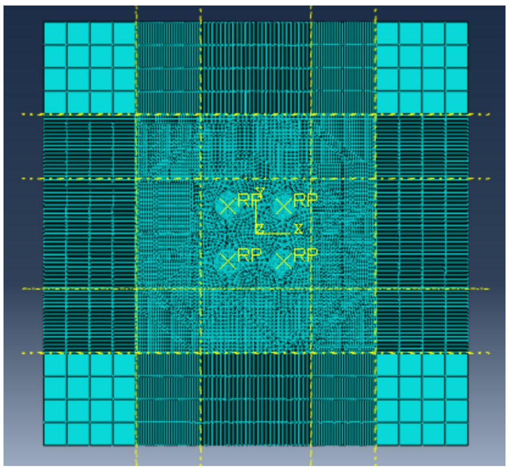

(a) Overview of element mesh

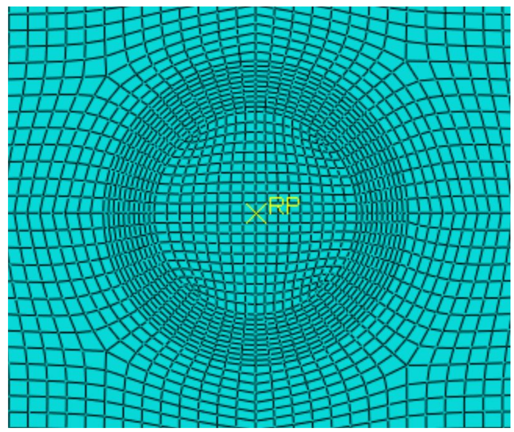

(b) Close up view of mesh around the piles

Figure 3.3: Element mesh

3.2 Model Validation

An isolated single pile is analyzed to verify the finite element model. To obtain a single pile the constraints on the other piles are removed. The remaining single pile is analyzed for multiple loading directions to ensure no mesh dependency with respect to loading direction exists. Figure 3.4 shows the p-y curves for a single isolated pile computed for different values of γ_{pf} and loading directions together with p-y curves from Zhang and Andersen (2017) (dashed lines). The single pile p-y curves from the FE analyses typically shows an ultimate bearing pressure of p_u from 12.75 to 12.9$s_u D$ depending on the pile group configuration and corresponding mesh. Compared to the theoretically exact solution of 11.94$s_u D$ (Randolph and Houlsby (1984)) for a flow-around mechanism, the finite element solution overestimates the ultimate bearing capacity with about 7%. Zhang and Andersen (2017) use N_p = 12 for a fully rough pile and the numerical overshoot can be seen in Figure 3.4. The numerical overestimation is due to discretization errors. Discretization error in FEA arises when the mesh density is too coarse. This will lead to an overly stiff solution and in turn overestimate the capacity. For this particular case, sufficient mesh refinement is especially a challenge in close proximity to the piles due to the curved geometry and large stress concentrations that occur in the area. However, the numerical error is expected to reduce when the p-y curve is normalised by the ultimate capacity.

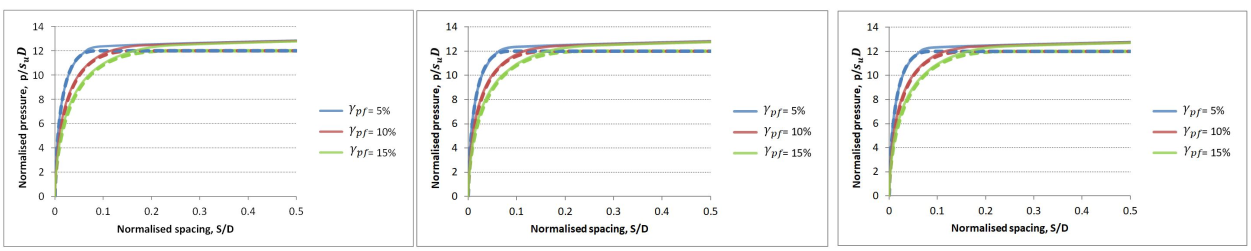

(a) $\omega = 0°$ (b) $\omega = 45°$ (c) $\omega = 90°$

Figure 3.4: Computed single pile p-y curves from FE (full lines) and Zhang and Andersen (2017) (dashed lines)

3.3 Determining p- and y-multipliers

3.3.1 P-multiplier

The p-multiplier is straightforwardly determined by dividing the ultimate lateral pressure $p_{u,i}$ for the group pile by the ultimate lateral pressure $p_{u,single}$ of the isolated single pile used for model validation:

$$p_{mod} = \frac{p_{u,i}}{p_{u,single}}$$

3.3.2 Y-multiplier

After the p-mulitplier has been determined the y-multiplier is calibrated. The y-multiplier is determined on a group basis. The total group p-y curve is obtained by plotting the displacement of the pile group and the sum of the lateral pressure of all n piles in the group:

$$p_{u,group} = \sum_{i=1}^{n} p_{u,i}$$

A representative group p-y curve from the isolated single pile (from model validation) is given by:

$$p_{u,group2} = n \cdot p_{u,single} \cdot p_{mod\,avg}$$

The two curves have the same ultimate lateral pressure p_u but different stiffness. The displacement values (y) of the stiffer p-y curve is multiplied by a constant value to match the stiffness of the actual group p-y curve. The value that gives the best match between the two p-y curves is taken as the y-multiplier value. It is not possible to achieve an exact point-by-point match of the curves utilizing a single y-multiplier value, but emphasis has been put on obtaining the best fit for the initial, stiffer parts of the curve (80 % of ultimate capacity).

Chapter 4

Results and discussions

This chapter presents the results of the parameter study. Functions to determine p- and y-multipliers based on pile spacing and loading angle is presented. The functions are given on the form $A|\sin B| + C$ and $a \sin b| + c$ for the p and y-multiplier, respectively. The six input parameters are specified for each pile group configuration.
The numerical results are compared with the existing method for determining p-multipliers as described in section 2.2.3. The comparison is made for two soil profiles: a lightly over-consolidated soil profile $s_u = 5.1 + 2.4z$ with $\gamma' = 7kN/m^3$ and a highly over-consolidated soil profile $s_u = 100kPa$ with $\gamma' = 10kN/m^3$ and two different pile diameters (D = 0.917 m and D = 2.00 m). Both suction and no suction conditions are considered.

4.1 Validation of Results for Varying stress-strain Response

The generality of the results presented in this chapter has been validated for three different stress-strain ranges by utilizing different values for the plastic shear strain at failure (γ_{pf} = 5%, γ_{pf} = 10% and γ_{pf} = 15%). Figure 4.1 shows the total group p-y curves for the 3-pile group (120°) configuration for two different spacing ratios (S/D = 2 and S/D = 3) and loading directions (ω = 90° and ω = 180°). The total ultimate group capacity is equal for all values of γ_{pf}. This confirms that the average group p-multipliers is valid for a general soil stress-strain relationship. As expected the displacement at which ultimate capacity is reached increase for higher values of γ_{pf}. For large group interaction effects (a loading direction of ω = 180° in this case) the pile displacement level that is required to reach convergence to ultimate capacity increase as the material behaviour becomes softer.

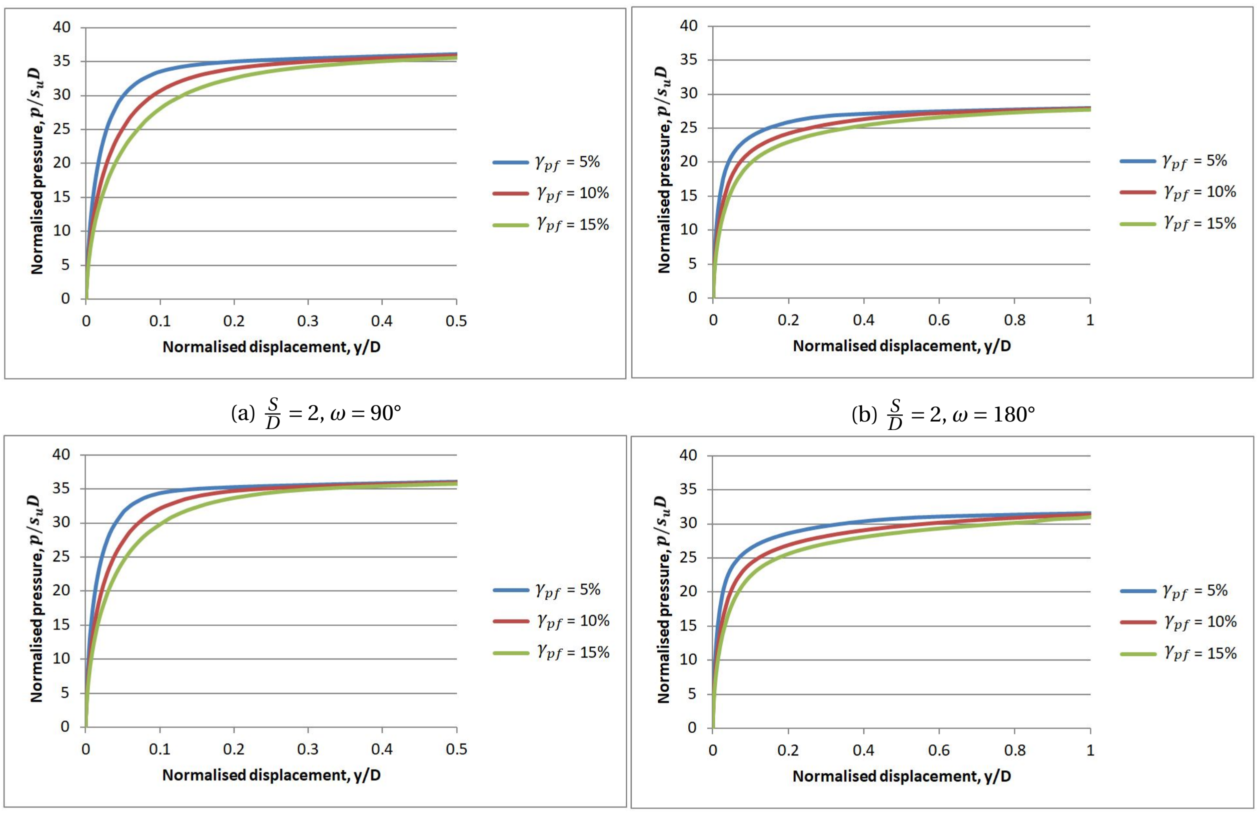

(a) $\frac{S}{D} = 2, \omega = 90°$

(b) $\frac{S}{D} = 2, \omega = 180°$

(c) $\frac{S}{D} = 3, \omega = 90°$

(d) $\frac{S}{D} = 3, \omega = 180°$

Figure 4.1: Ultimate group capacity for different values of γ_{pf}

Figure 4.2 shows the total computed pile group capacity of the 3-pile group (120 °) for S/D = 2 and ω = 90° and different values of γ_{pf}. The red curve represents the group response computed from 3 single p-y curves while the blue curve represent the actual group response. The red curve is multiplied by the average group p-multiplier and a group y-multiplier. The red and blue curve show a perfect match for all γ_{pf} using the same values for the group p-multiplier and group y-multiplier in all cases. This confirms that the y-multipliers is valid for a general soil stress-strain relationship.

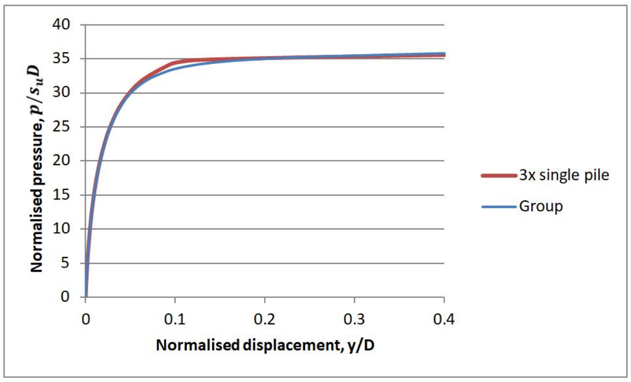

(a) $\gamma_{pf} = 5\%$

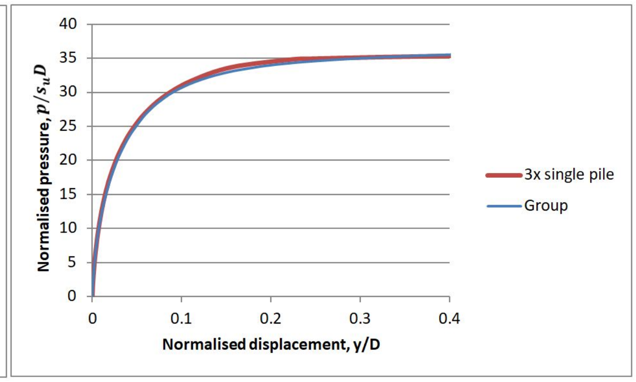

(b) $\gamma_{pf} = 10\%$

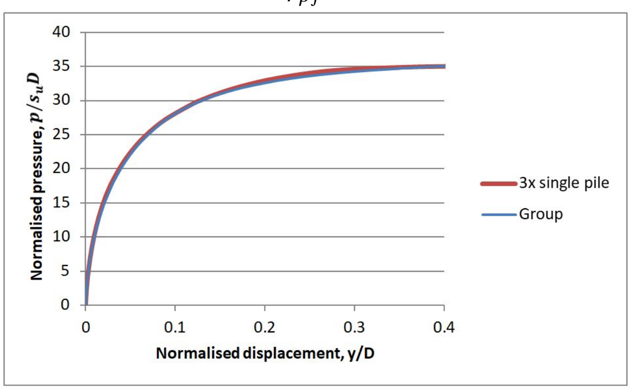

(c) $\gamma_{pf} = 15\%$

Figure 4.2: Group p-y curves computed from single pile p-y curves and actual group response for different γ_{pf}

4.2 2-pile group

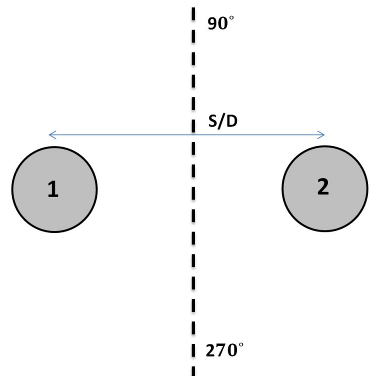

Figure 4.3: 2-pile group

Figure 4.4 shows the resulting normalised p-y curves for different loading directions ω and pile spacing ratios S/D. The response of both piles are identical because a flow-around mechanism is simulated. In a flow-around mechanism both piles mobilize an active and passive zone and there is no difference in the response between leading or trailing piles.

Figure 4.4 shows that the group interaction effects are largest for a loading direction of $\omega = 0°$ in which the shear zones overlap the most. For a loading direction $\omega = 90°$ the shear zones extend in parallel and little overlapping occurs, which consequently results in less reduction of stiffness and bearing capacity. As the spacing ratio S/D increases the pile group experience less reduction of lateral bearing capacity. However, reduction in stiffness is still prominent even for the largest pile spacing S/D = 5.

Figure 4.5 shows the resulting group y-multiplier. The stiffness is not sensitive to S/D and it is only dependent on the loading angle ω.

Note that the capacity of the piles for S/D = 2 and loading direction $\omega = 90°$ is almost equal to the single pile (red curve) and higher than the capacity for the same loading direction for S/D = 3. This is examined further by exploring the displacement contours in Figure 4.6

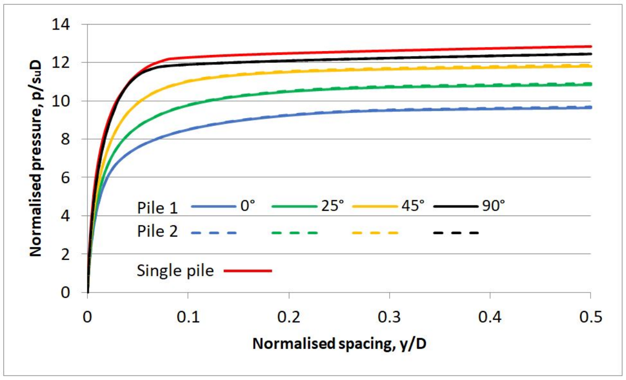

(a) $\frac{S}{D}$=2

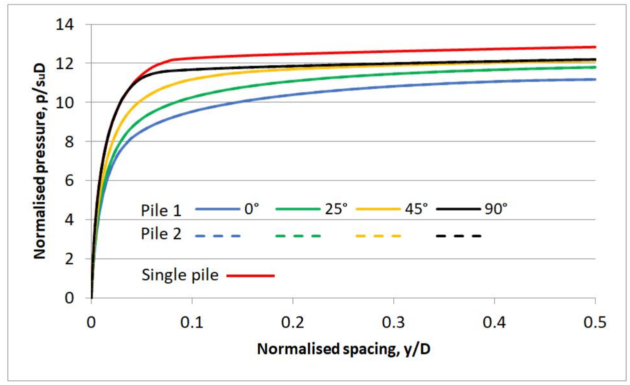

(b) $\frac{S}{D}$=3

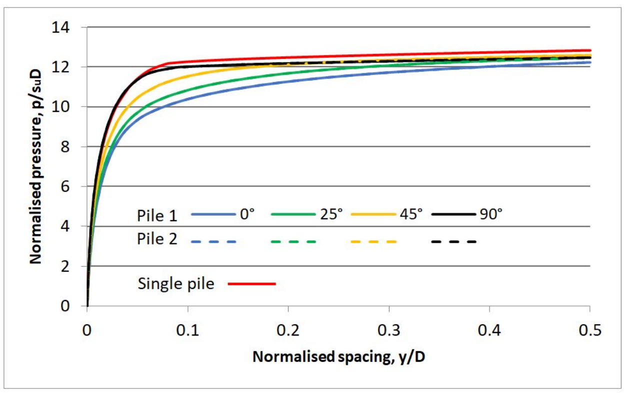

(c) $\frac{S}{D}$=4

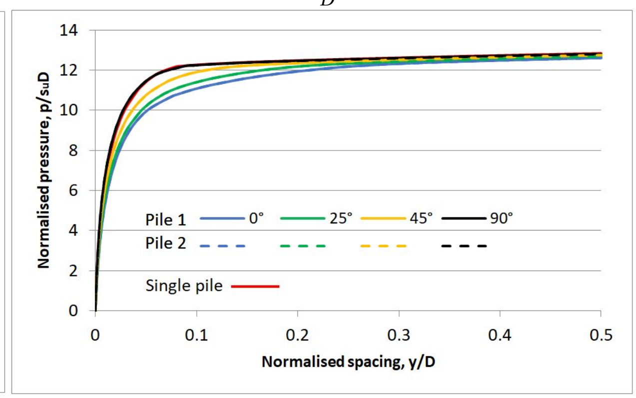

(d) $\frac{S}{D}$=5

Figure 4.4: Normalised p-y curves (S/D = 2,3,4,5). The red curve show the single isolated pile response

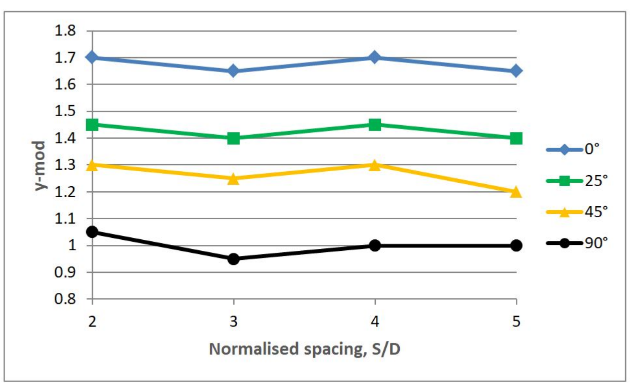

(a) Variation of y-multiplier with pile spacing

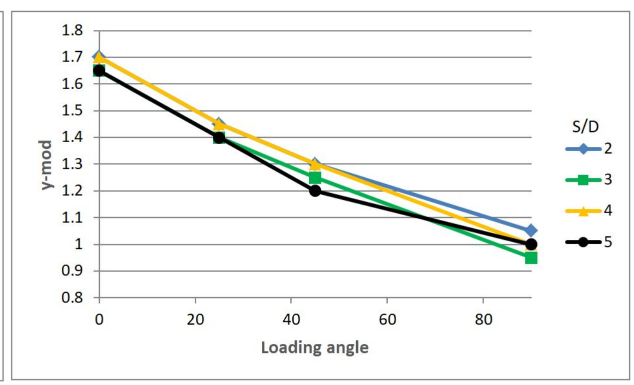

(b) Variation of y-multiplier with loading direction

Figure 4.5: y-multiplier 2-pile group

Figure 4.6shows the displacement contours for loading direction ω = 90° of a single pile and the 2-pile group for S/D = 1.25, 2 and 3. Only half of the pile group is shown because of symmetry conditions. The flow-around displacement zone from Randolph and Houlsby (1984) can be recognized for the single pile. Interaction can be seen to take place between the piles. Outside the piles (to the left of the pile the figure) the area of mobilized soil are larger for S/D = 1.25 and S/D = 2 compared to S/D = 3. For S/D ≤ 2 the two piles resemble a larger pile and enable mobilization of a larger soil volume. Mobilizing displacement in a greater soil volume requires more force and in turn provide larger lateral bearing resistance. However, the beneficial interaction is lost as S/D exceeds 2.

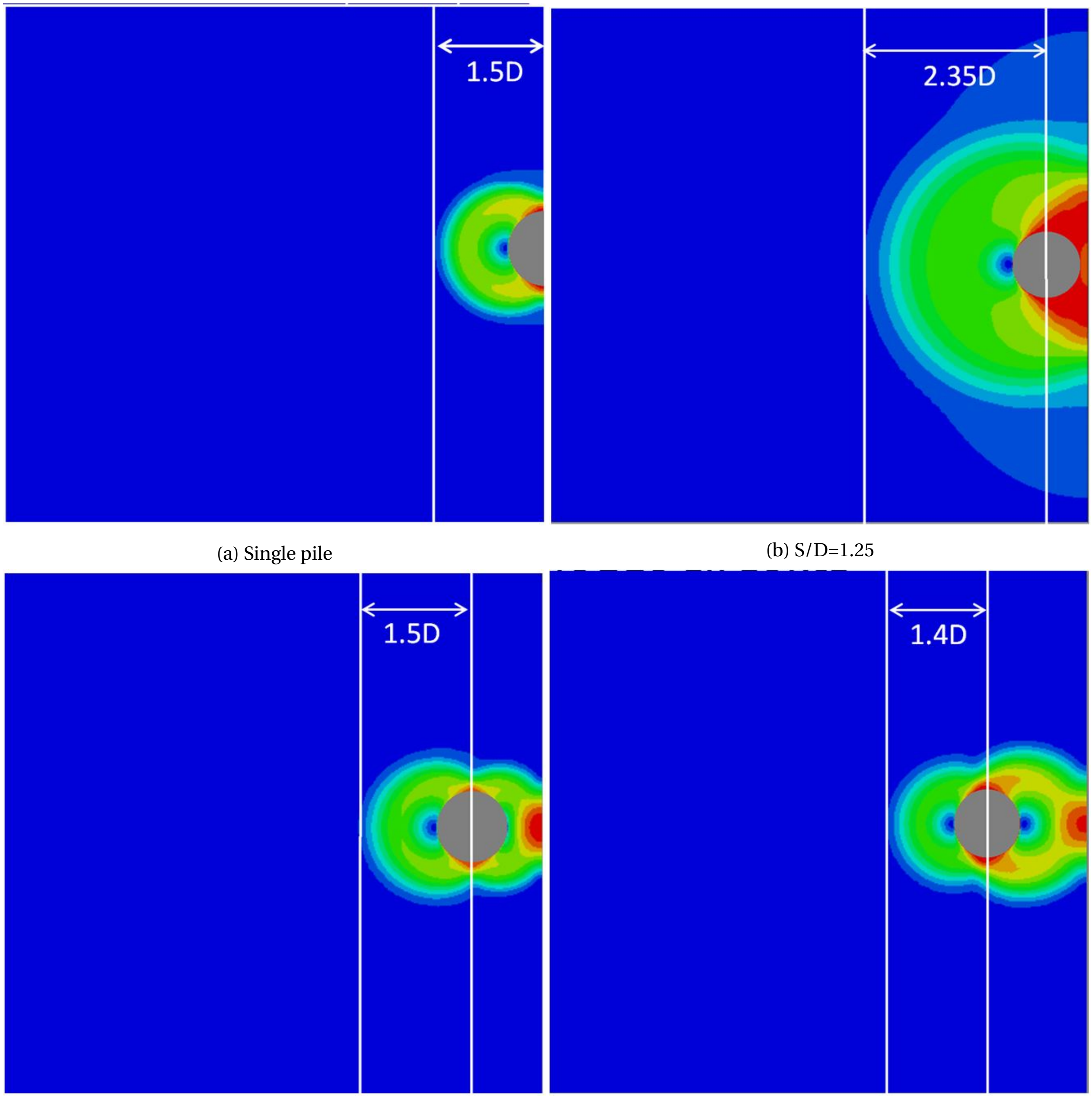

(a) Single pile

(b) S/D=1.25

(c) S/D=2

(d) S/D=3

Figure 4.6: Displacement contours for a single pile and 2-pile group with S/D = 1.25, 2 and 3 for $\omega = 90°$

4.2.1 Functions for Determining Group p- and y-multipliers

The proposed functions for determining the group p- and y-multiplier is presented in Table 4.1. The proposed function for the p-multiplier (dashed lines) is compared with the group p-multiplier from the FE results (dots) in Figure Figure 4.7. The proposed function for the y-multiplier (dashed lines) is compared with the group y-multiplier from the FE results (dots) in Figure Figure 4.8.

Table 4.1: Functions for p- and y-multipliers 2-pile group

p_{mod}: A$\lvert\sin B\rvert$+C	y_{mod}: a$\lvert\sin b\rvert$+c
A = $0.033\left(\frac{S}{D}\right)^2 - 0.3\left(\frac{S}{D}\right) + 0.7$	a = -0.75
B = ω	b = ω
C = $-0.023\left(\frac{S}{D}\right)^2 + 0.24\frac{S}{D} + 0.36$	c = 1.75

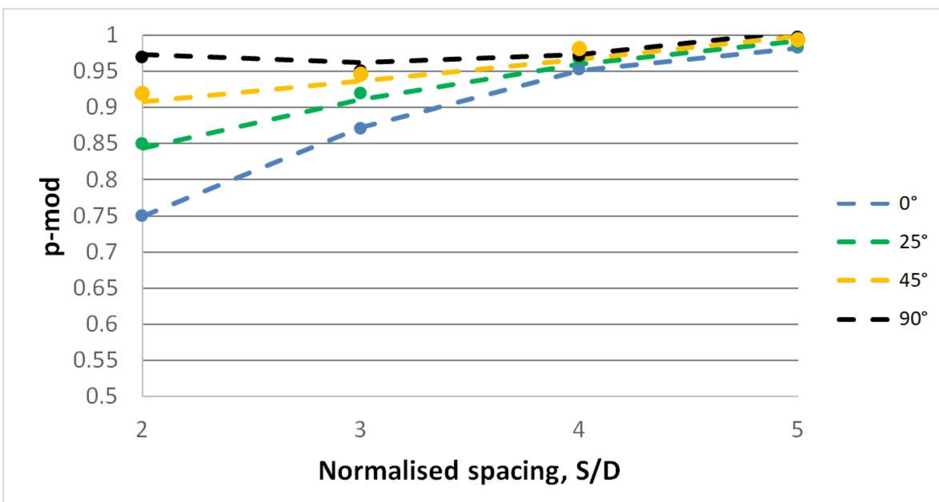

Figure 4.7: Proposed function for p_{mod} (dashed lines) vs FE results (dots)

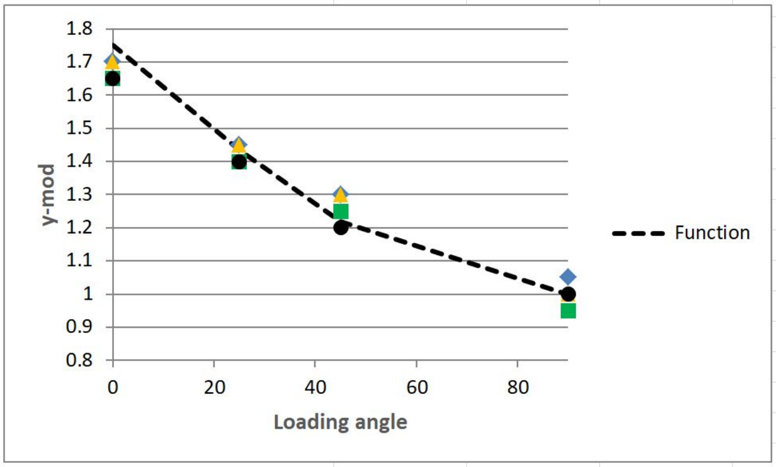

Figure 4.8: Proposed function for y_{mod} (dashed lines) vs FE results (dots)

4.2.2 Comparison with existing method

Figure 4.9 and Figure 4.10 shows the comparison between the finite element results and the existing method for suction and no suction conditions, respectively. As the p-multiplier from the finite element analysis is dependent on the loading direction, the boundary values are presented in the figure where the leftmost line represents $\omega = 0°$ and the rightmost $\omega = 90°$.

For $\omega = 0$ the FE results are more conservative for all S/D and both suction conditions. For $\omega = 90$ the existing method is more conservative for S/D = 2 while the results are fairly similar for larger pile spacings. The area of an equivalent pier for a 2-pile group is not that large resulting in an equivalent diameter that is not considerable larger compared to the actual pile diameter. The existing approach will thus not give a lot of reduction in capacity.

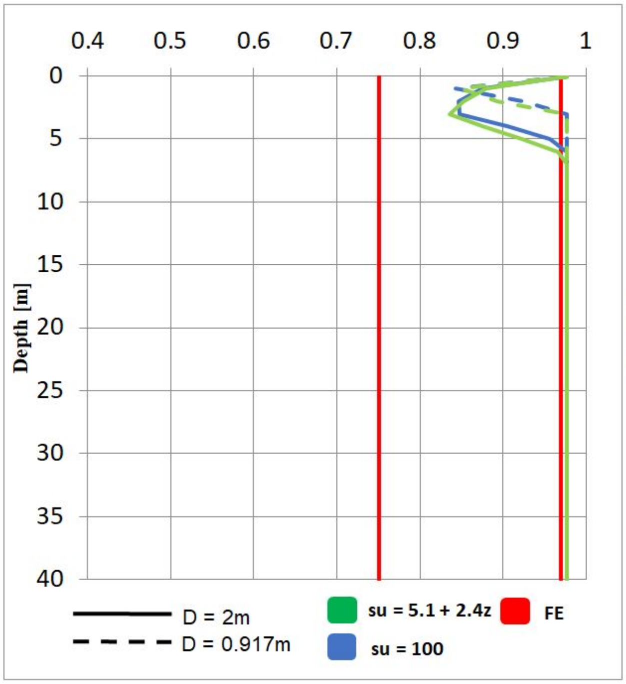

(a) S/D = 2

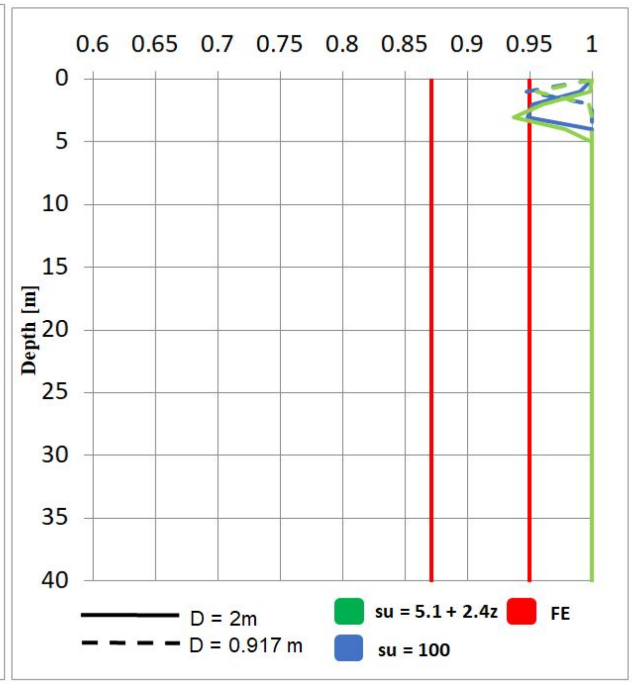

(b) S/D = 3

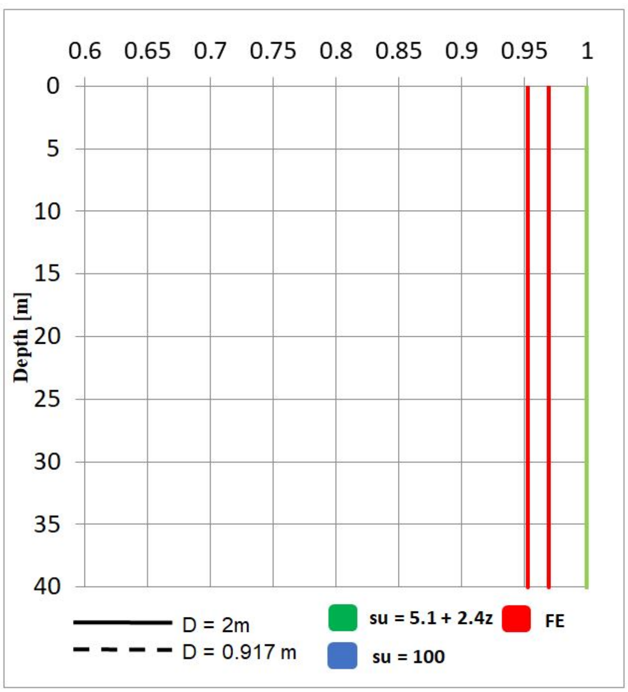

(c) S/D = 4

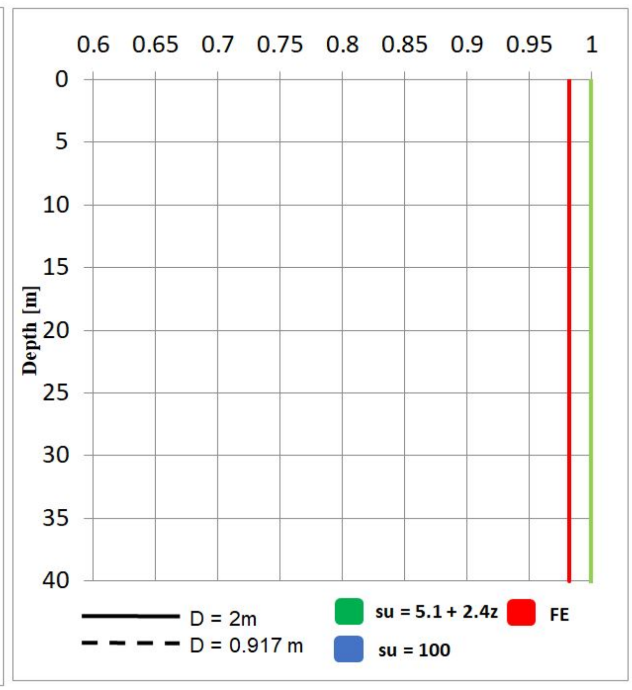

(d) S/D = 5

Figure 4.9: Comparison of p-multiplier with existing method 2-pile group. No gap

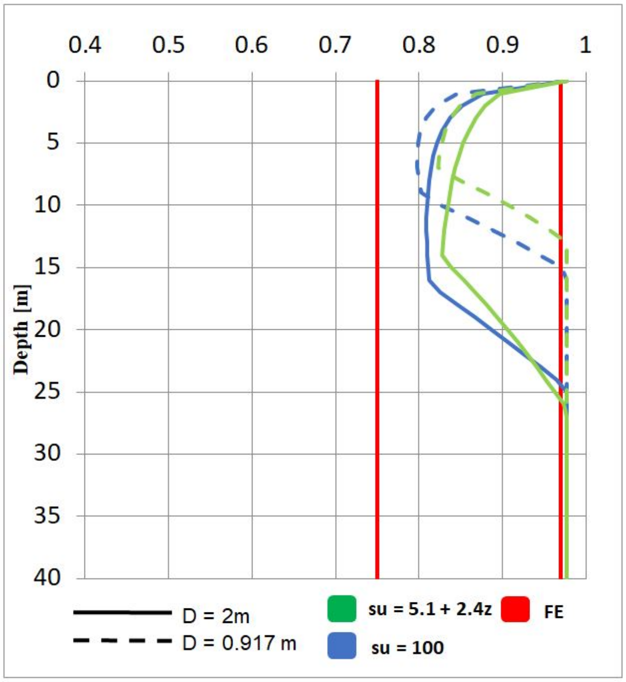

(a) S/D = 2

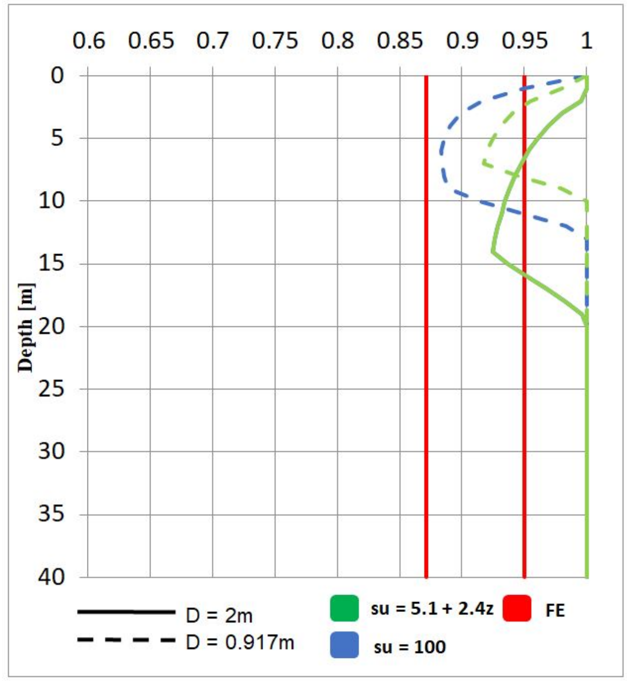

(b) S/D = 3

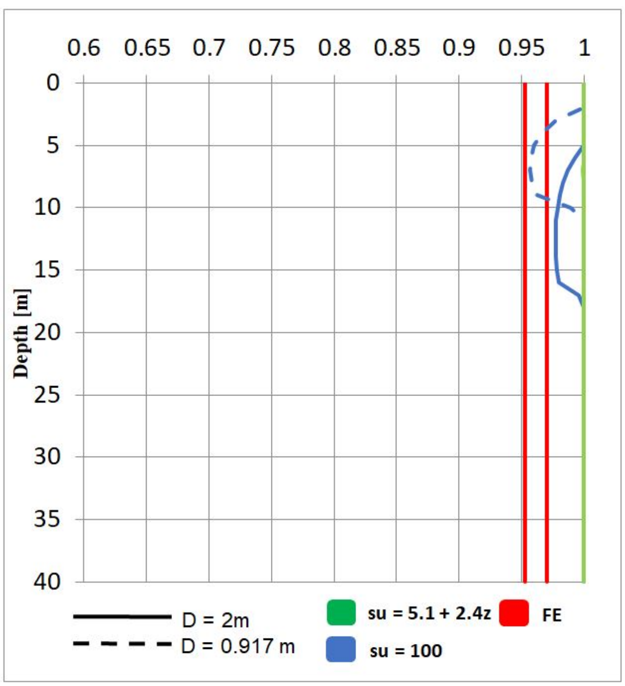

(c) S/D = 4

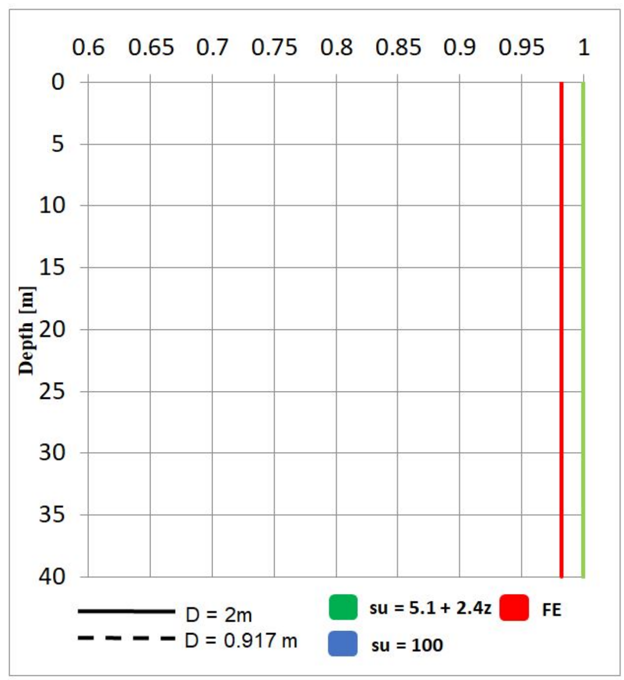

(d) S/D = 5

Figure 4.10: Comparison of p-multiplier with existing method 2-pile group. With gap

4.3 3-pile group (90 ° triangle)

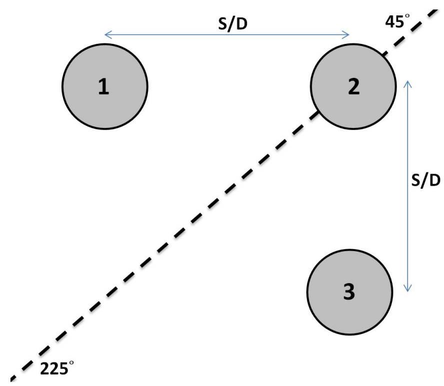

Figure 4.11: 3-pile group (90 ° triangle

4.3.1 Results

Figure 4.12 shows the resulting p-multipliers for the different piles. The p-multiplier increase with S/D and is close to unity (0.985) for S/D = 5. The average group group p-multiplier is not very sensitive to the loading angle and can be approximated as constant for all values of ω.

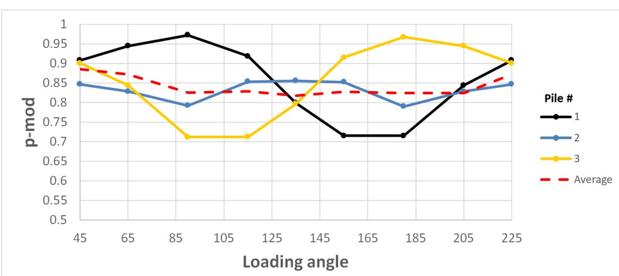

(a) $\frac{S}{D}$=2

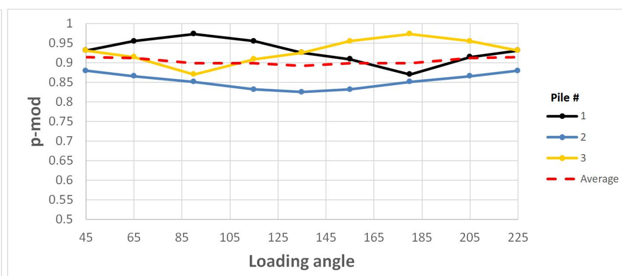

(b) $\frac{S}{D}$=3

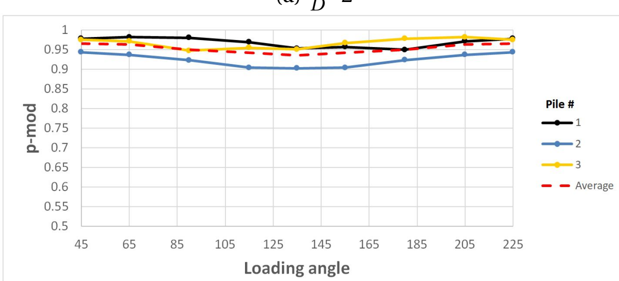

(c) $\frac{S}{D}$=4

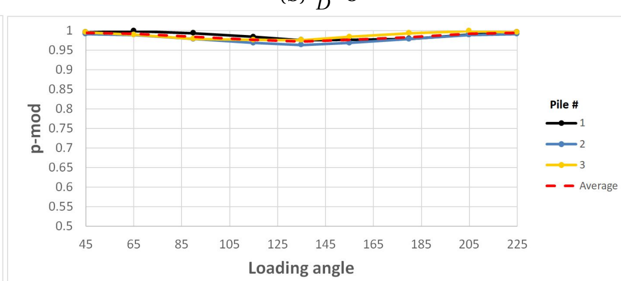

(d) $\frac{S}{D}$=5

Figure 4.12: P-multiplier for 3-pile group (90 ° triangle) (S/D = 2,3,4,5)

Figure 4.13 shows the resulting group y-multiplier. The pile group stiffness is sensitive to both S/D and loading angle ω.

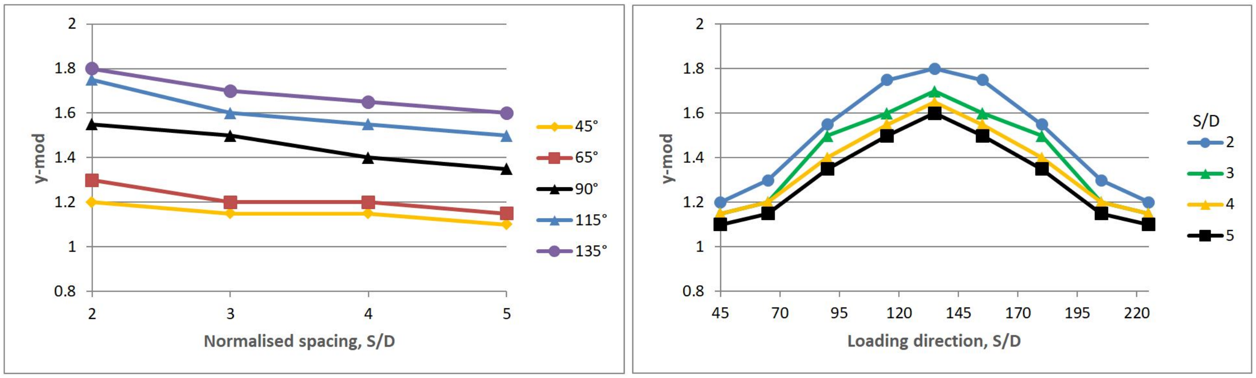

(a) Variation of y-multiplier with pile spacing

(b) Variation of y-multiplier with loading direction

Figure 4.13: y-multiplier 3-pile group (90° triangle)

The p-multiplier curve for pile 1 & 3 has the shape of a double-wave. The curves are equivalent in shape but shifted 90 degrees relative to each other, corresponding to the angle between the piles. The p-multiplier for pile 2 has the shape of a single wave and is generally lower than pile 1 & 3 for S/D > 2. However, there is a notable difference in the response of the piles for S/D = 2 compared to S/D ≥ 3. For S/D = 2 the curve for pile 2 is higher than the curve for pile 1 (for $\omega \in$ [65 - 135 degrees]) and pile 3 (for $\omega \in$ [135 - 205 degrees]). Moreover, pile 2 has its maximum bearing capacity at 135° for S/D = 2, while pile 2 has its lowest bearing capacity at 135° for S/D > 2. This is explored further by studying the displacement contours for S/D = 2 and 3 for loading directions ω = 90° and ω = 135°.

Figure 4.14 shows that pile 2 displaces a much larger soil volume for S/D = 2 compared to S/D = 3. This is particularly clear for ω = 135° and explains why pile 2 has a higher relative capacity compared to the other piles for S/D = 2. However, the group p-multiplier is still lowest for the S/D = 2 and there is no overall beneficial group effect as was observed in the 2-pile group case.

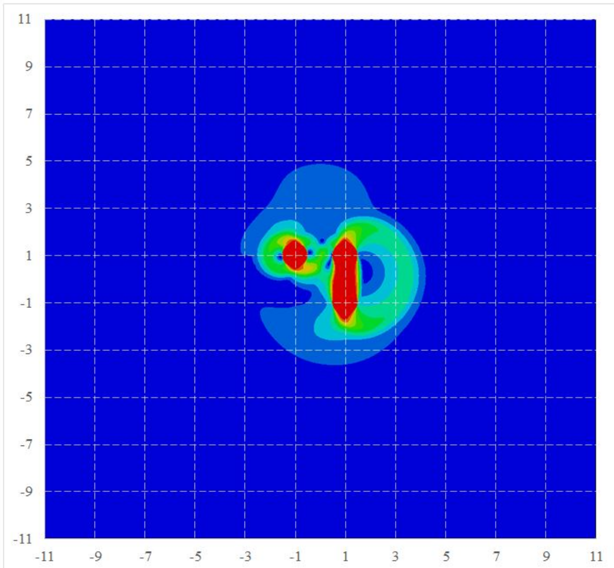

(a) $\frac{S}{D}$=2 $\omega = 90°$

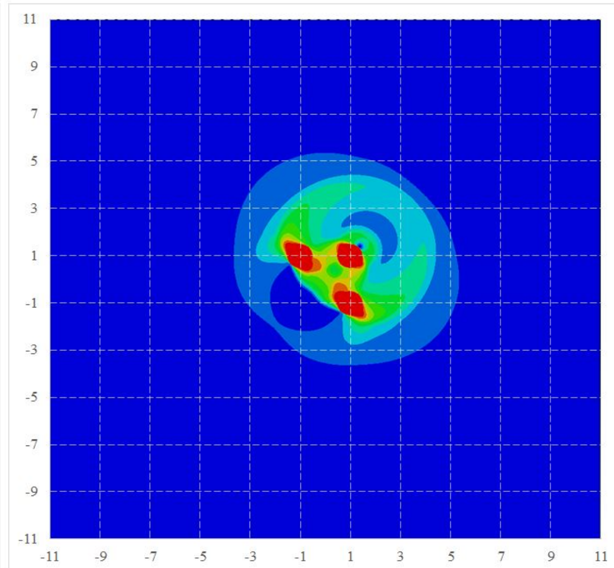

(b) $\frac{S}{D}$=2 $\omega = 135°$

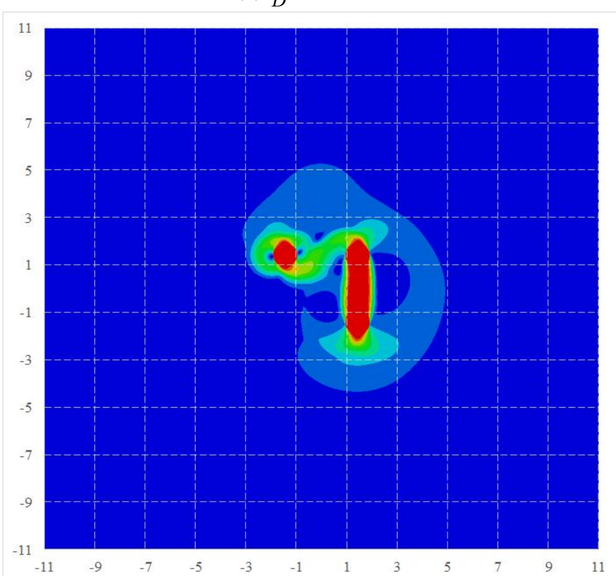

(c) $\frac{S}{D}$=3 $\omega = 90°$

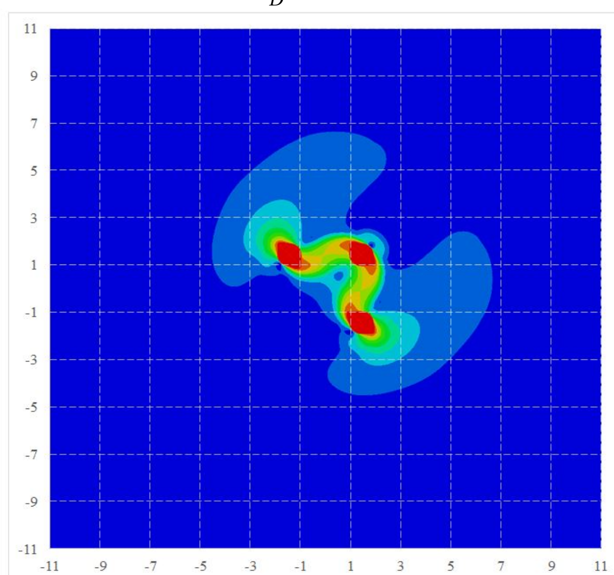

(d) $\frac{S}{D}$=3 $\omega = 135°$

Figure 4.14: Displacement contours for 3-pile group (90°)

4.3.2 Functions for Determining Group p- and y-multipliers

The proposed function for determining the group p- and y-multiplier is presented in Table 4.2. The proposed function (dashed lines) for the p-multiplier is compared with the average group p-multiplier from the FE results (red dots) in Figure 4.15. The red dots are the average of the average of the p-multiplier from Figure 4.12 for different S/D. The proposed function for the y-multiplier (dashed lines) is compared with the group y-multiplier from the FE results (dots) in Figure Figure 4.16.

Table 4.2: Functions for p- and y-multipliers 3-pile group (90 ° triangle)

p_{mod} A$\|\sin B\|$+C	y_{mod} a$\|\sin b\|$+c
$A = 0.05\frac{S}{D}$	$a = -0.065\frac{S}{D} + 0.80$
$B = \pi/2$	$b = \omega - \pi/4$
$C = 0.75$	c=1.1

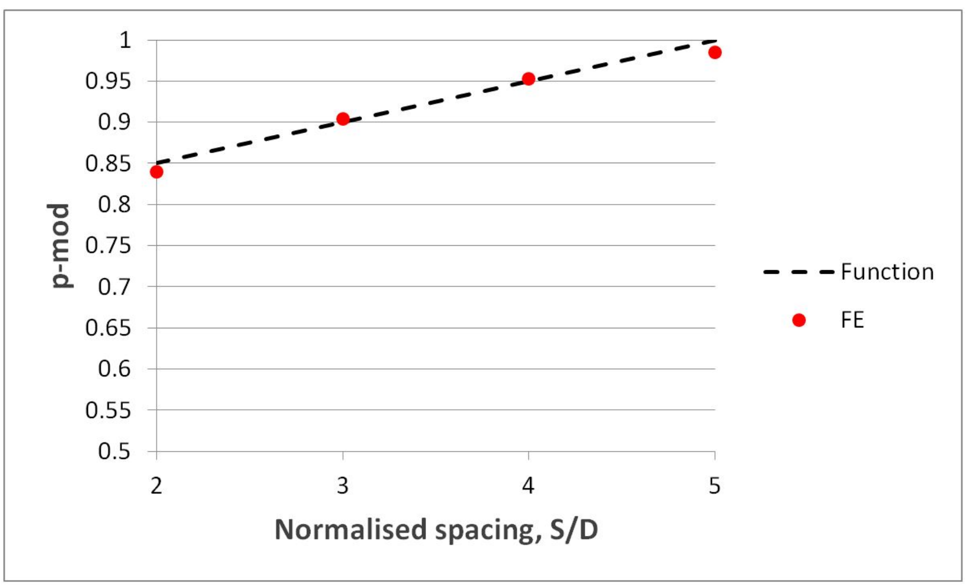

Figure 4.15: Proposed function for p_{mod} (dashed lines) vs FE results (dots)

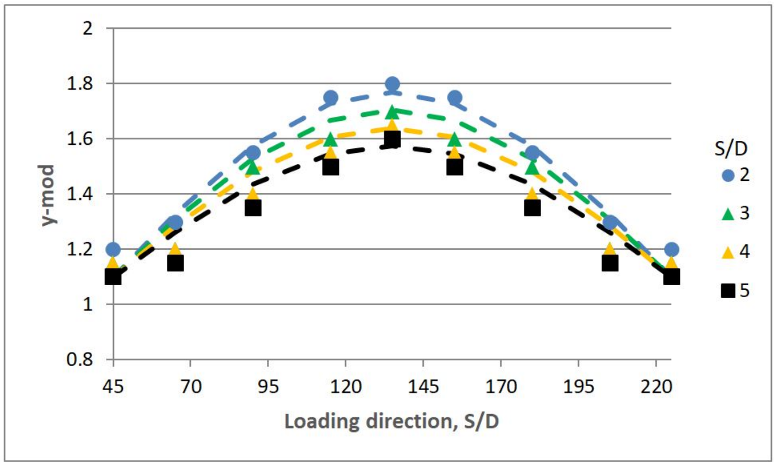

Figure 4.16: Proposed function for y_{mod} (dashed lines) vs FE results (dots)

4.3.3 Comparison with existing method

Figure 4.17 and Figure 4.18 compares the finite element (FE) results with the existing method for suction and no suction conditions, respectively. For S/D = 2 the existing method is conservative for both suction conditions and the maximum deviation between the methods is 0.19. With no gap the FE results are generally more conservative for S/D > 2. With gap the existing method is generally more conservative for S/D = 3. For S/D = 4 the existing method is only conservative for heavily overconsolidated soil while for S/D = 5 the FE results are overall more conservative.

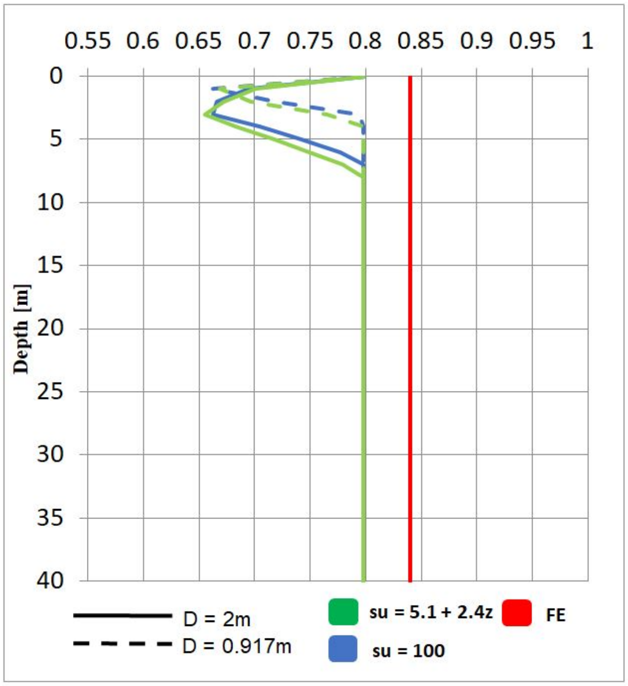

(a) S/D = 2

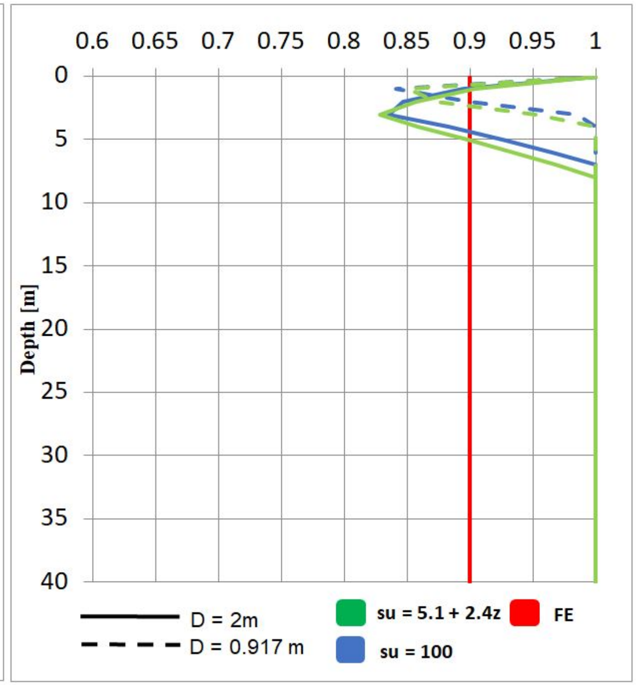

(b) S/D = 3

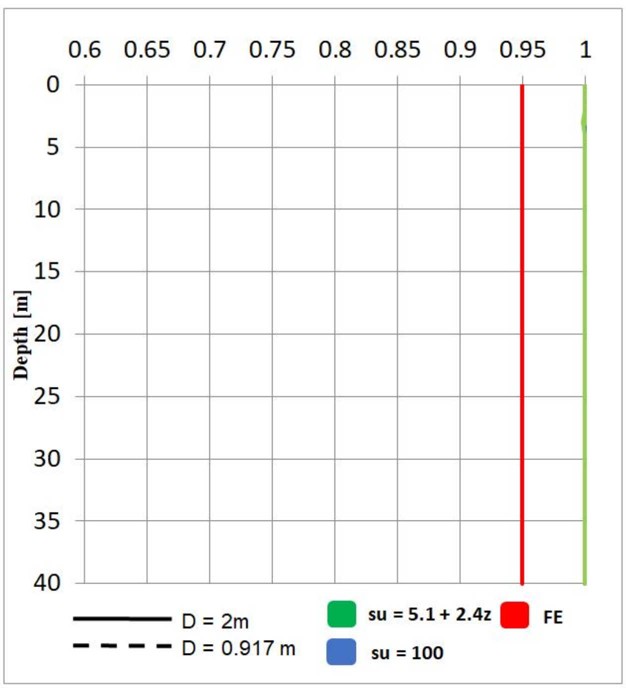

(c) S/D = 4

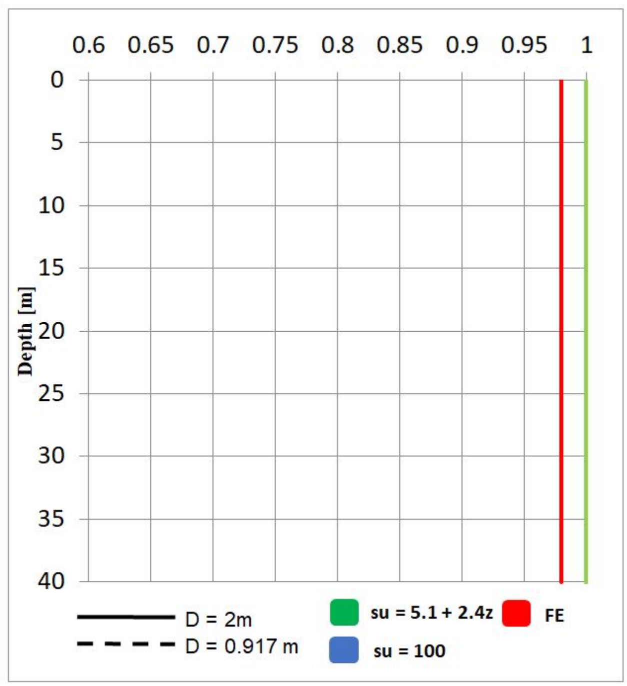

(d) S/D = 5

Figure 4.17: Comparison of p-multiplier with existing method 3-pile group (90°) No gap

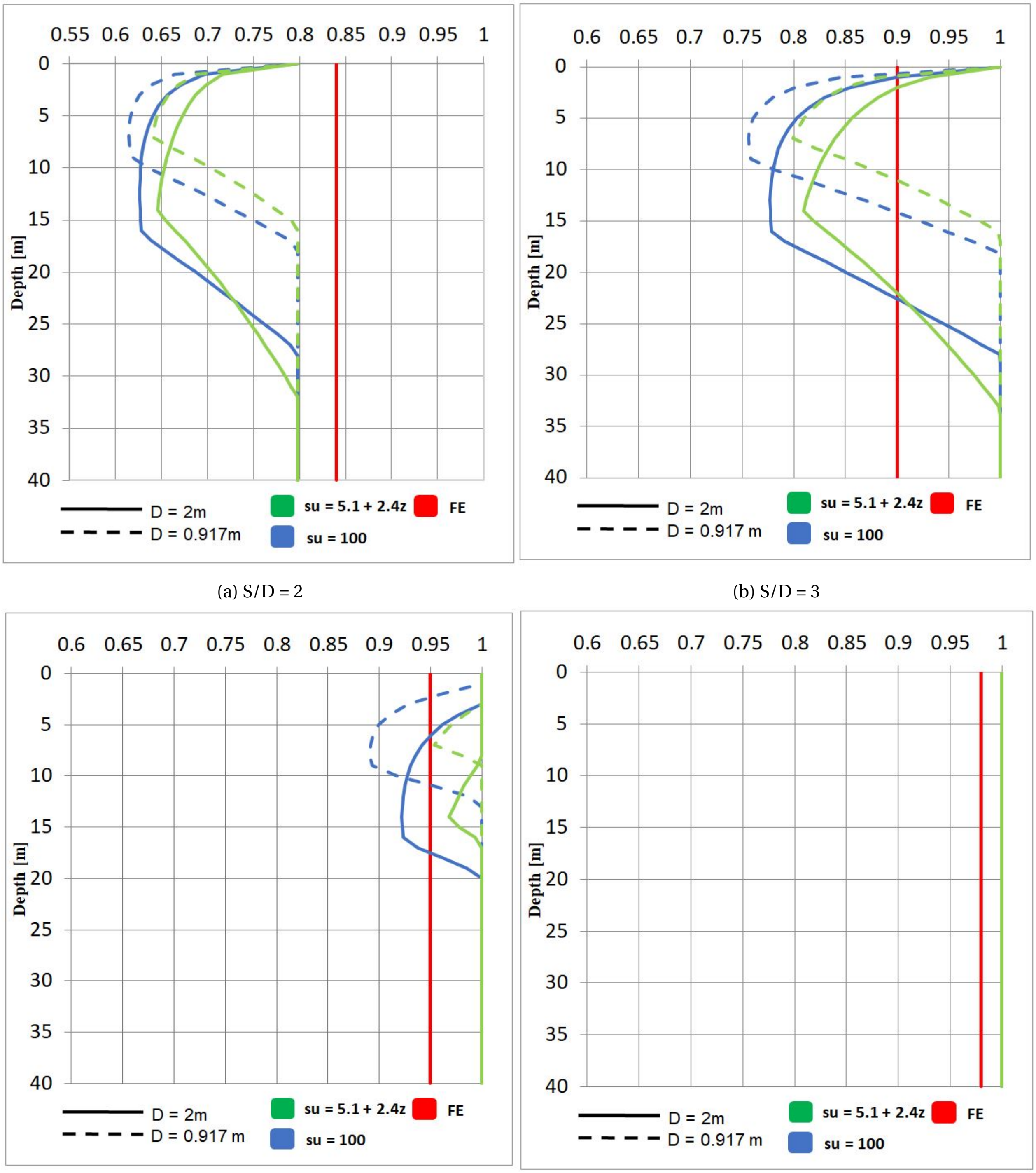

(a) S/D = 2

(b) S/D = 3

(c) S/D = 4

(d) S/D = 5

Figure 4.18: Comparison of p-multiplier with existing method 3-pile group (90°). With gap

4.4 3-pile group (equilateral triangle)

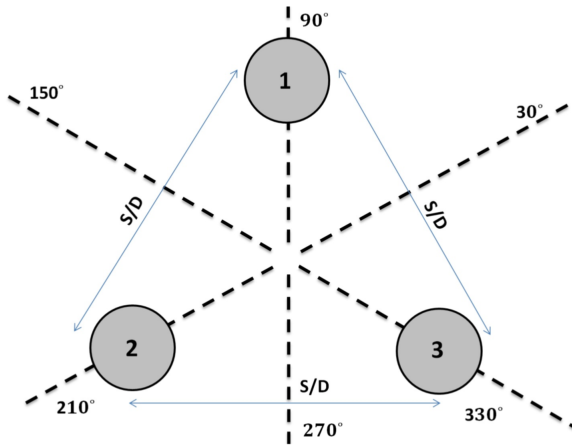

Figure 4.19: 3-pile group (equilateral triangle)

4.4.1 Results

Figure 4.20 shows the resulting p-multipliers for the different piles. The p-multiplier increase with S/D and is close to unity (0.985) for S/D = 5. The average group group p-multiplier is not very sensitive to the loading direction and can be approximated as constant for all values of ω

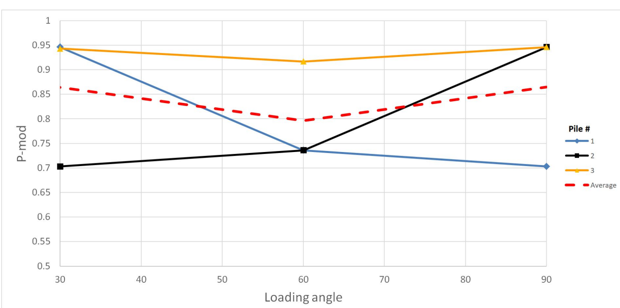

(a) $\frac{S}{D}$=2

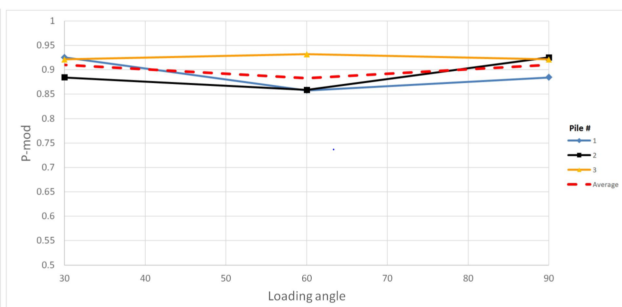

(b) $\frac{S}{D}$=3

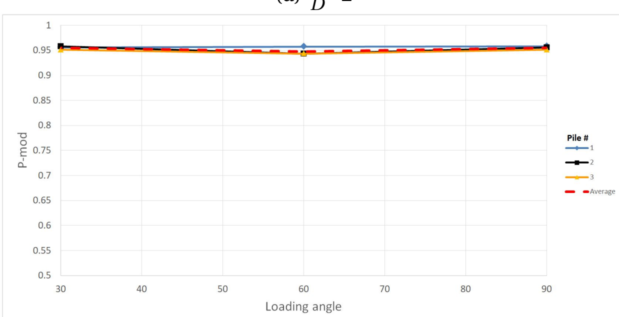

(c) $\frac{S}{D}$=4

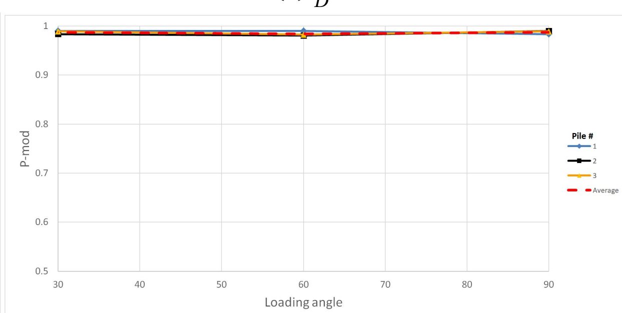

(d) $\frac{S}{D}$=5

Figure 4.20: P-multiplier for 3-pile group (equilateral) (S/D = 2,3,4,5)

Figure 4.21 shows the group y-multiplier. The pile group stiffness is independent of both S/D and loading angle ω in the interval of interest (S/D = 2-5). However, additional analyses of S/D = 8 shows that the stiffness will increase for S/D ratios beyond the scope of this study. Because the pile group has 3 lines of symmetry with a span of merely 60 °, it is expected that the lateral response is not affected to a large extent by the loading direction.

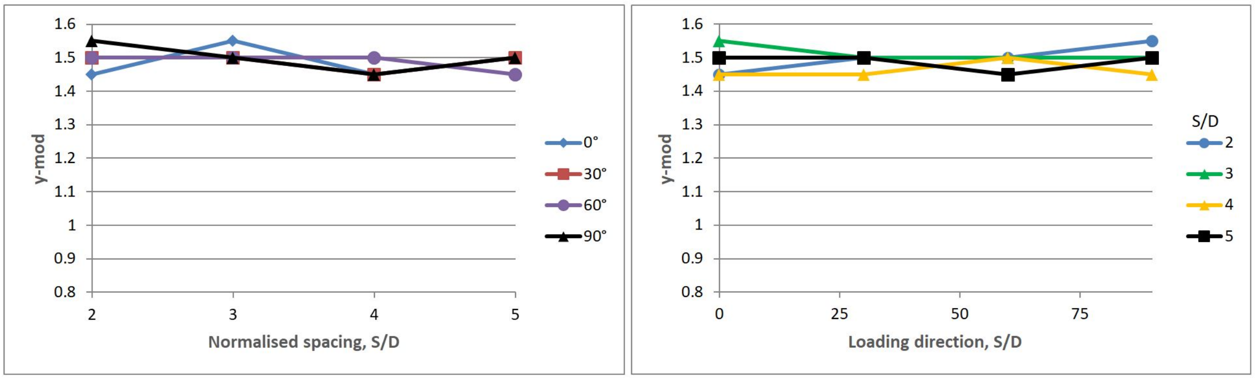

(a) Variation of y-multiplier with pile spacing

(b) Variation of y-multiplier with loading direction

Figure 4.21: Functions for p- and y-multipliers (equilateral triangle)

4.4.2 Functions for Determining Group p- and y-multipliers

The proposed functions for determining the group p- and y-multiplier presented in Table 4.3. The values for the average group p-multiplier for different values of S/D is almost identical to that of the 3-pile group (90°) and the same function can be used to predict the p-multiplier for both pile group configurations. The proposed function for the p-multiplier is compared with the FE results in **??**.

Table 4.3: p- and y-multiplier expression for 3-pile group (equilateral triangle)

p_{mod} A$\|\sin B\|$+C	y_{mod} a$\|\sin b\|$+c
A = $0.05\frac{S}{D}$	a=0
B = $\pi/2$	b=0
C = 0.75	c=1.5

4.4.3 Comparison with existing method

Figure 4.23 and Figure 4.24 compares the finite element (FE) results with the existing method for suction and no suction conditions, respectively. For S/D = 2 the existing method is very conservative for both suction conditions.

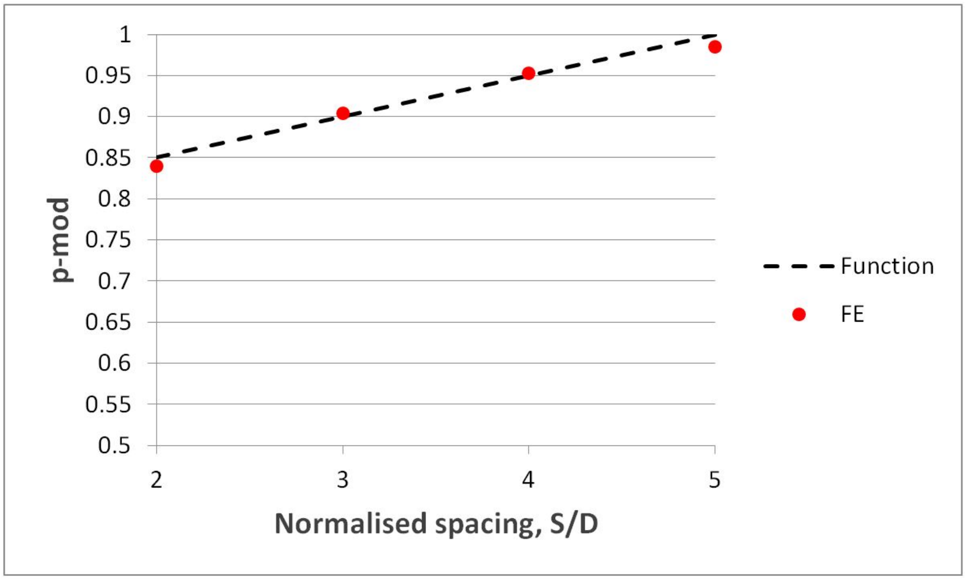

Figure 4.22: Proposed function for p-mod vs FE results

With no gap the the FE results are generally more conservative, except for the upper parts. With gap the existing method is more conservative for S/D = 3 and S/D = 4 while there is not much deviation for S/D = 5.

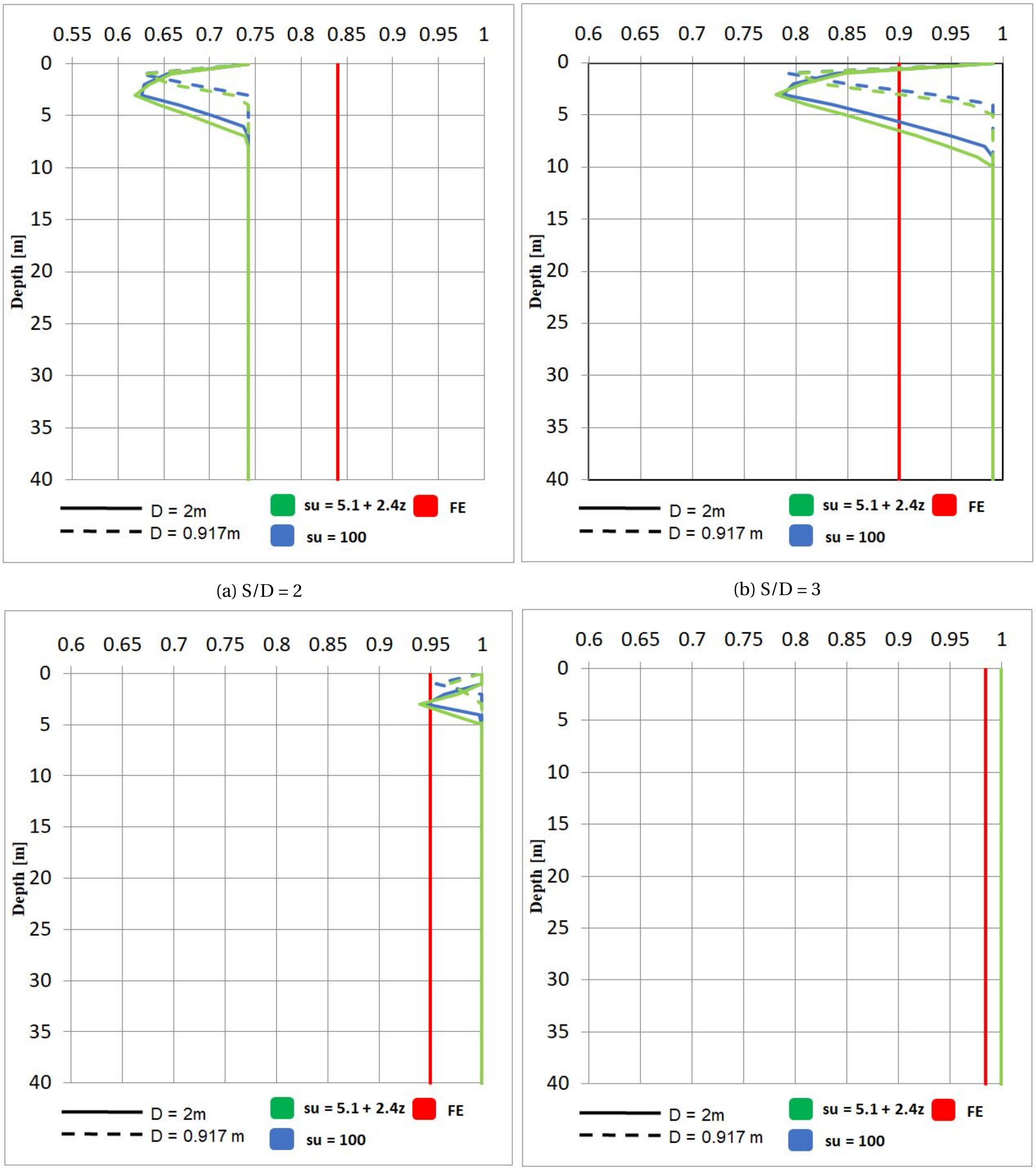

(a) S/D = 2

(b) S/D = 3

(c) S/D = 4

(d) S/D = 5

Figure 4.23: Comparison of p-multiplier with existing method 3-pile group (equilateral). No gap

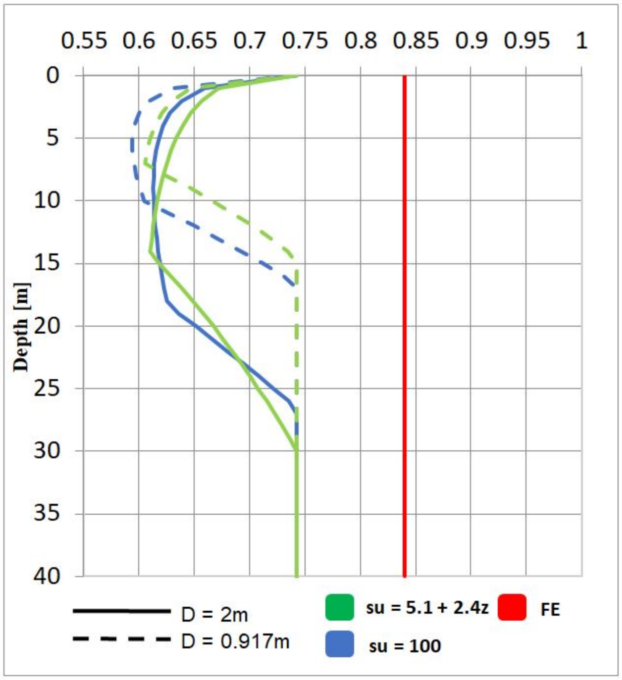

(a) S/D = 2

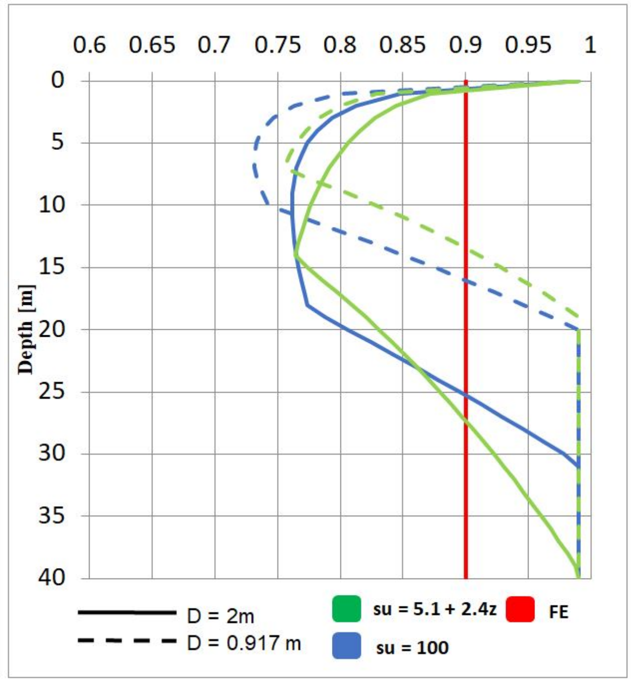

(b) S/D = 3

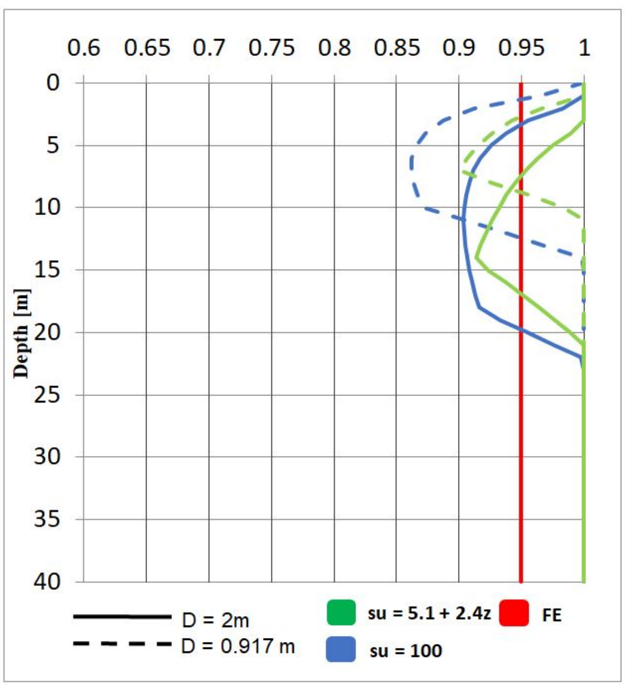

(c) S/D = 4

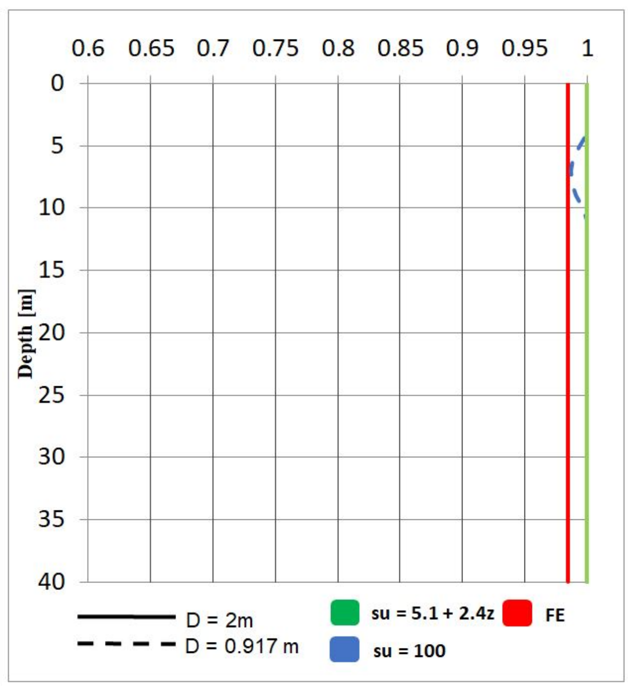

(d) S/D = 5

Figure 4.24: Comparison of p-multiplier with existing method 3-pile group (equilateral). With gap

4.5 3-pile group (120 ° triangle)

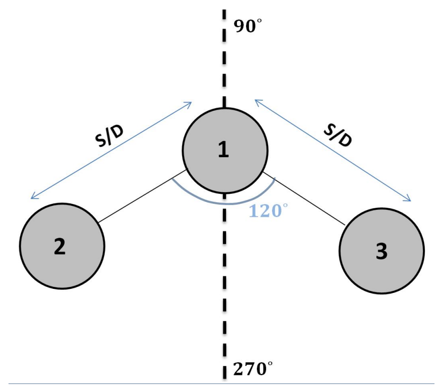

Figure 4.25: 3-pile group (120 ° triangle)

4.5.1 Results

Figure 4.26 shows the resulting p-multipliers for the different piles. The p-multiplier increase with S/D and is close to unity (0.95-1.00) for S/D = 5. The group p-multiplier is dependent on the loading direction. This is contrary to the other 3-pile group configurations in which the average group p-multiplier was not sensitive to the loading direction. The shear zone overlapping of the middle pile (1) and two side piles (2 & 3) is a lot more prominent for a loading direction of 180° compared to 90°. Consequently there is a large relative difference in group interaction effects between different loading directions, similar to the 2-pile group.

Figure 4.27 shows the resulting y-modifier for the pile group. The pile group stiffness increase from S/D = 2 to S/D = 3, but is not very sensitive to further increase in S/D. The pile group stiffness is also sensitive to the loading direction

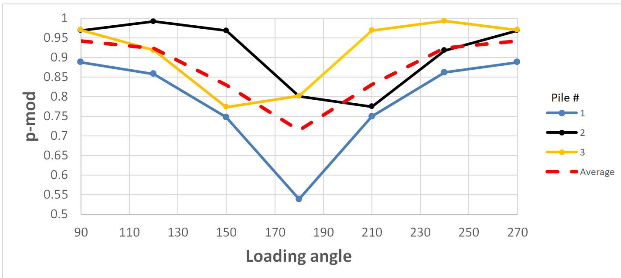

(a) $\frac{S}{D}$=2

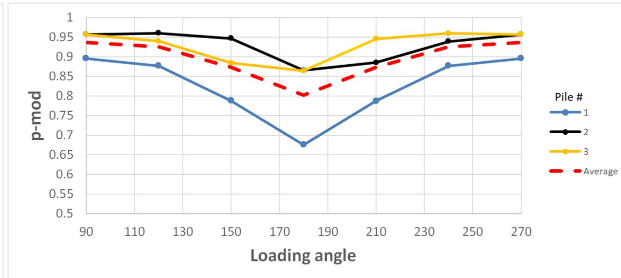

(b) $\frac{S}{D}$=3

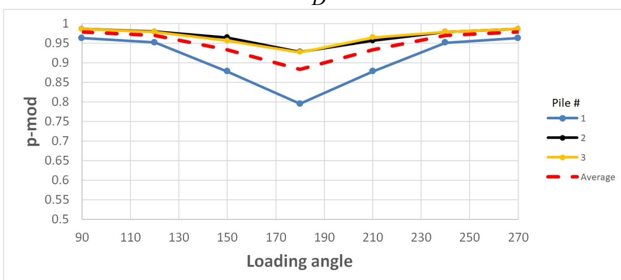

(c) $\frac{S}{D}$=4

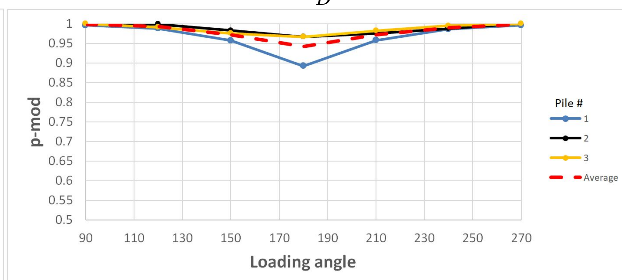

(d) $\frac{S}{D}$=5

Figure 4.26: P-multiplier for 3-pile group (120 deg) (S/D = 2,3,4,5)

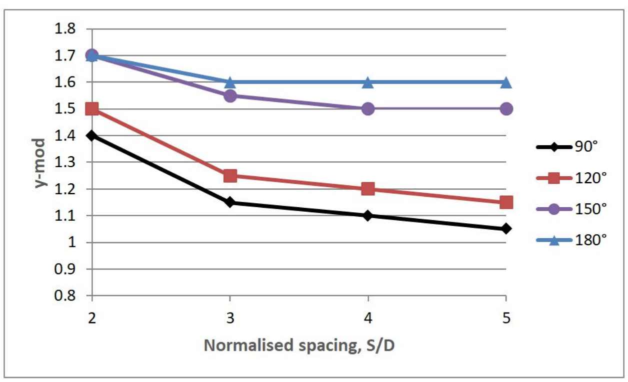

(a) Variation of y-multiplier with pile spacing

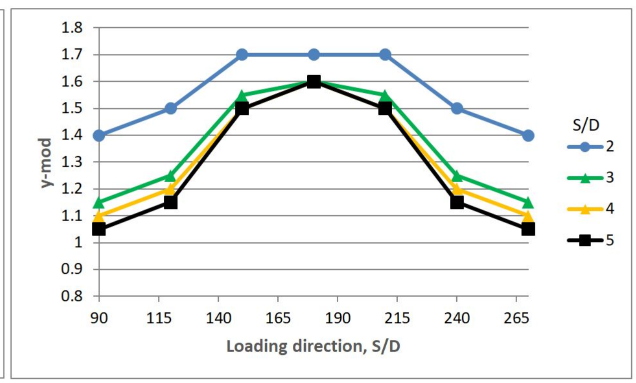

(b) Variation of y-multiplier with loading direction

Figure 4.27: y-multiplier 3-pile group (120° triangle)

Figure 4.29 illustrate the variation in group p-multiplier for different loading directions ω and spacing ratios S/D. For ω = 90° the group p-multiplier is higher for S/D = 2 than for S/D = 3. This is due to the same phenomenon as was explored in the 2-pile group case. Figure 4.28 shows the displacement contours at ω = 90° for S/D = 2 and S/D = 3. For S/D = 2 the pile group is able to mobilize more soil volume outside the piles compared to S/D = 3, thus indicating a beneficial group interaction resulting in increased capacity. However, the capacity is only slightly higher for S/D = because there are still negative group interaction occurring between the piles.

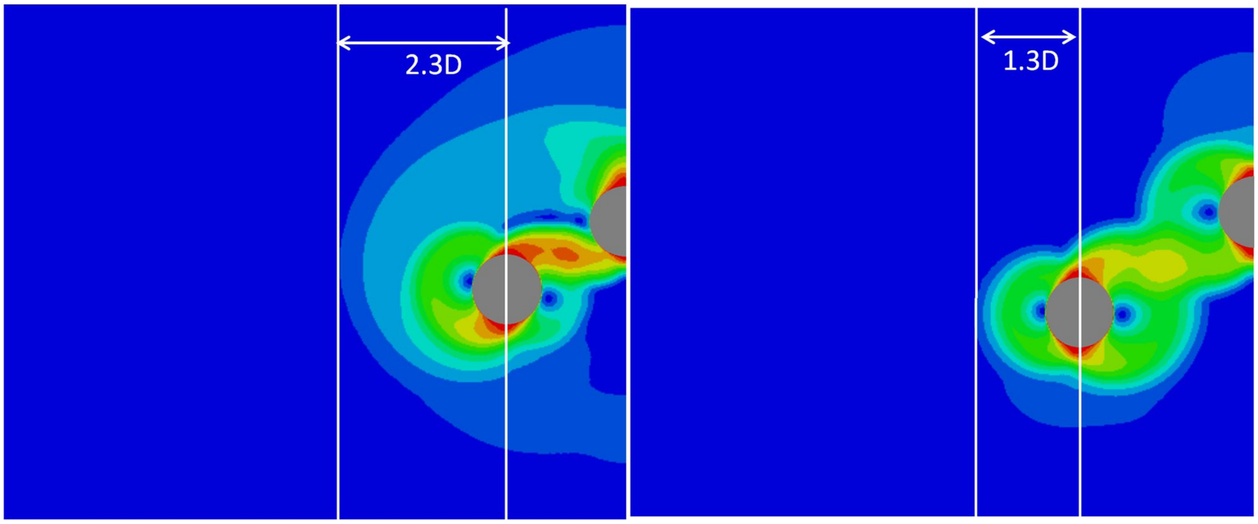

(a) S/D = 2, $\omega = 90$

(b) S/D = 3, $\omega = 90$

Figure 4.28: Displacement field for 120 degree pile group (S/D = 3)

4.5.2 Functions for Determining Group p- and y-multipliers

The proposed functions for determining the group p- and y-multiplier is presented in Table 4.4. The proposed function for the group p-multiplier (dahsed lines) is compared with the FE results in Figure 4.29. The proposed function for the y-multiplier (dashed lines) is compared with the group y-multiplier from the FE results (dots) in Figure Figure 4.30.

Table 4.4: Functions for p- and y-multipliers for 3-pile group (120 ° triangle)

p_{mod} A$\lvert \sin B \rvert$+C	y_{mod} a$\lvert \sin b \rvert$+c
$A = 0.317 - 0.054\frac{S}{D}$	a = $\begin{cases} 0.3, & S/D = 2, \\ 0.5, & S/D > 2. \end{cases}$
$B = \omega$	b=ω-$\pi/2$
$C = 0.072\frac{S}{D} + 0.58$	a = $\begin{cases} 1.4, & S/D = 2, \\ 1.1, & S/D > 2. \end{cases}$

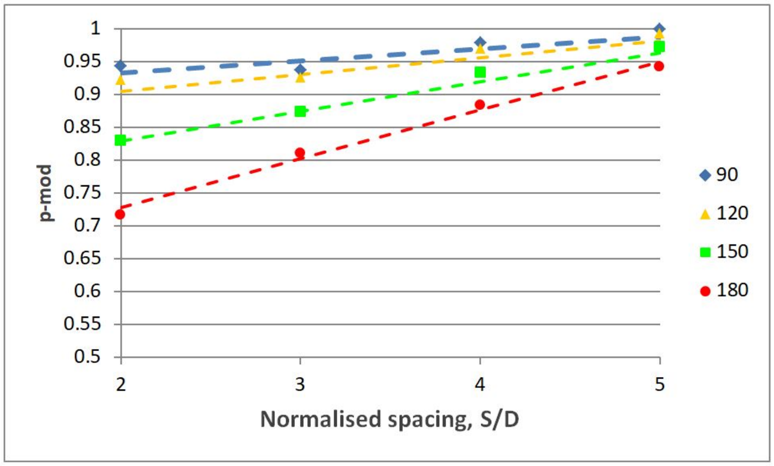

Figure 4.29: Proposed function for p_{mod} (dashed lines) vs FE results (dots)

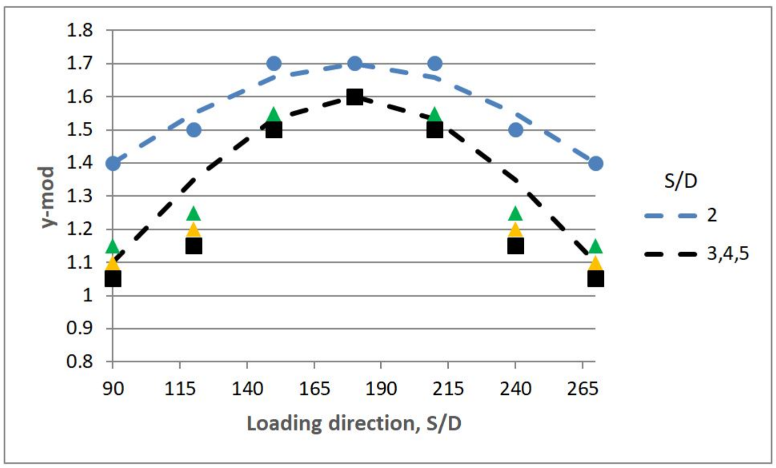

Figure 4.30: Proposed function for y_{mod} (dashed lines) vs FE results (dots)

4.5.3 Comparison with existing method

Figure 4.31 and Figure 4.32 compares the finite element results (FE) with the existing method for suction and no suction conditions, respectively. As the p-multiplier from the finite element analysis is dependent on the loading direction, the boundary values are presented in the figure where the leftmost line represents ω = 180° and the rightmost ω = 90°.

For S/D = 2 the existing method is more conservative for both suction conditions. The deviation becomes particularly large for ω = 90° as the FE results give almost no reduction for this loading direction while the existing method predicts an overall reduction of over 40%.

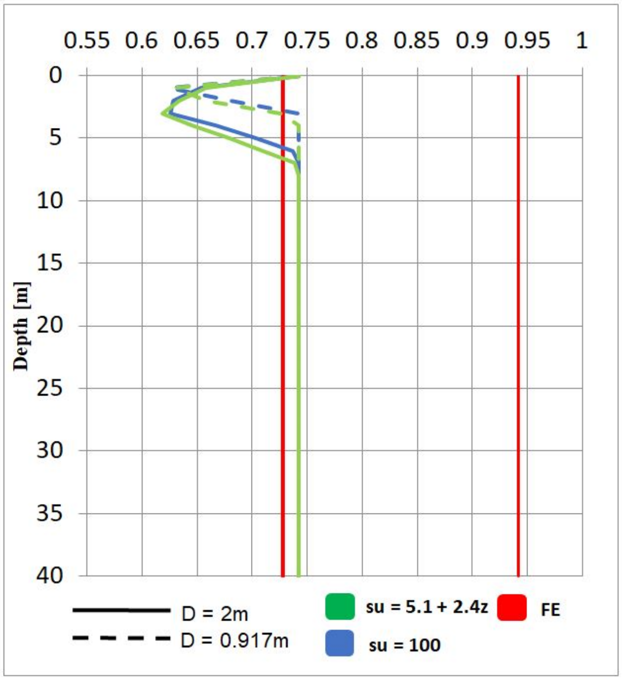

(a) $\frac{S}{D} = 2$

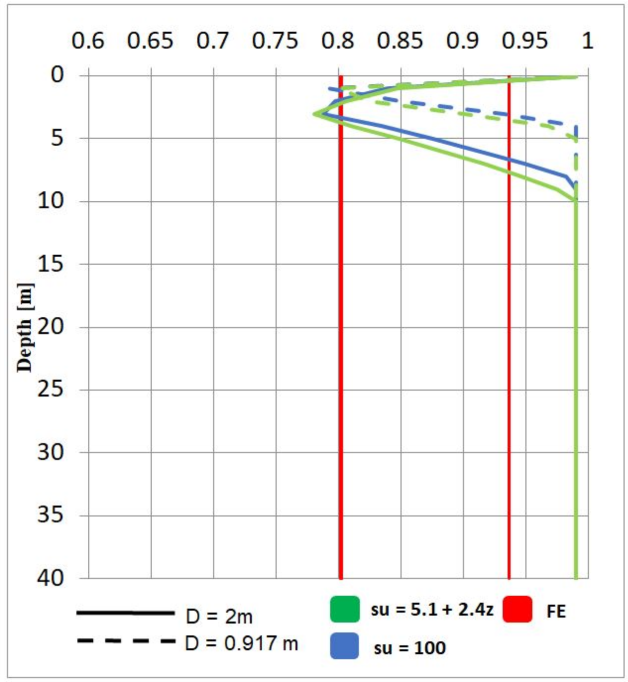

(b) $\frac{S}{D} = 3$

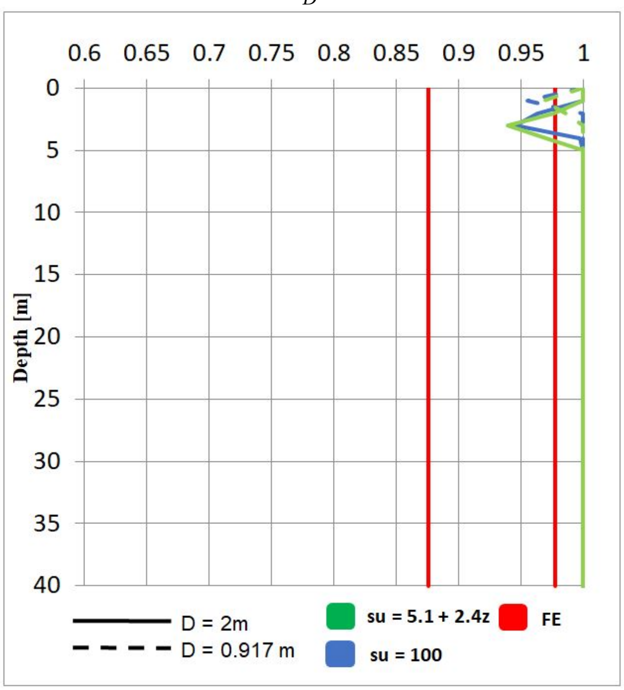

(c) $\frac{S}{D} = 4$

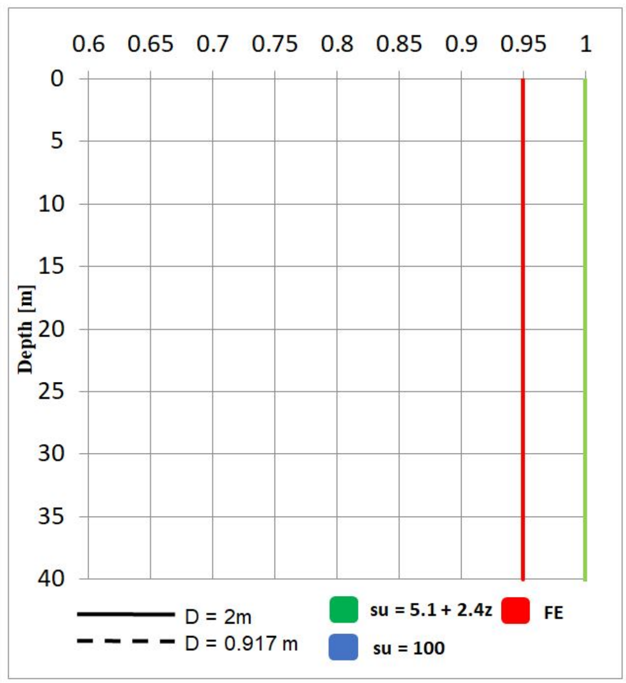

(d) $\frac{S}{D} = 5$

Figure 4.31: Comparison of p-multiplier with existing method 3-pile group (120°). No gap

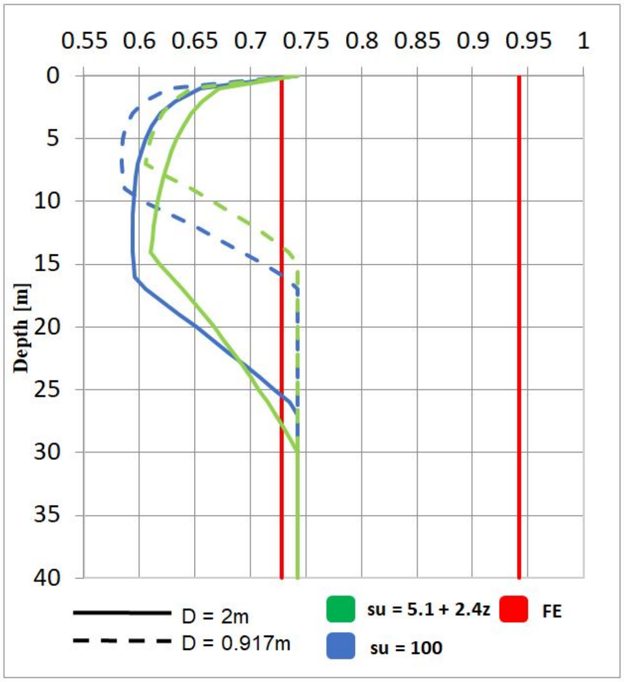

(a) $\frac{S}{D} = 2$

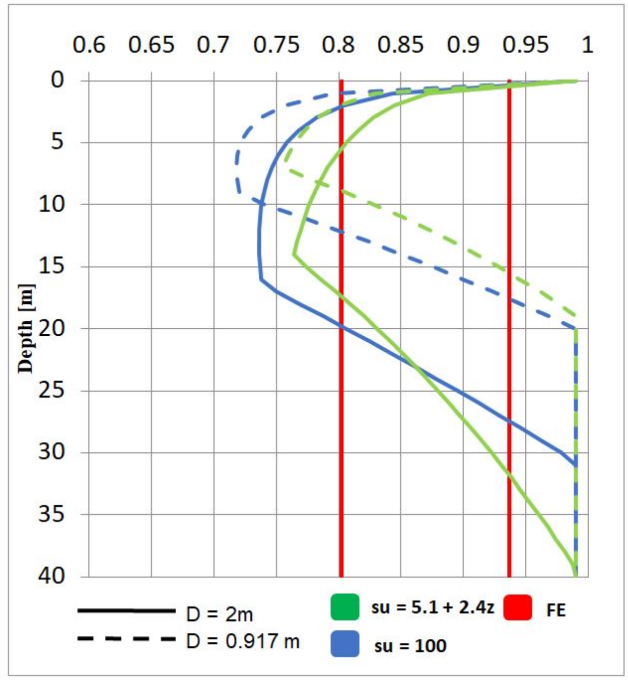

(b) $\frac{S}{D} = 3$

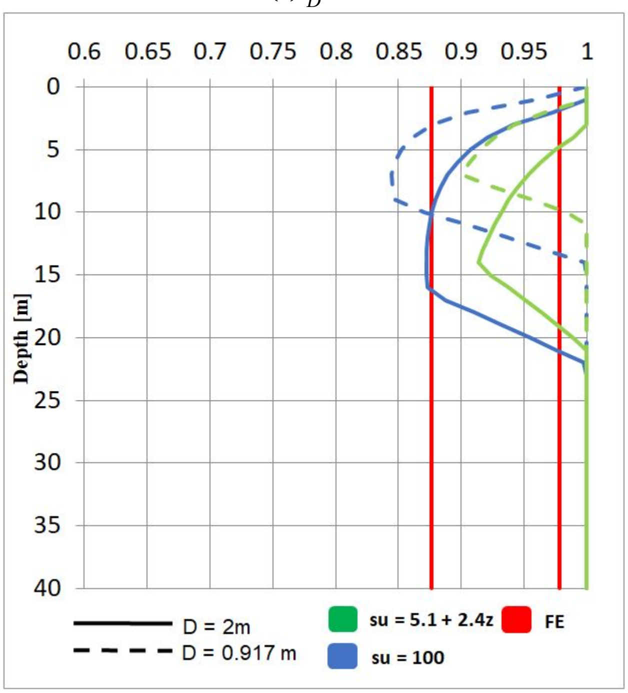

(c) $\frac{S}{D} = 4$

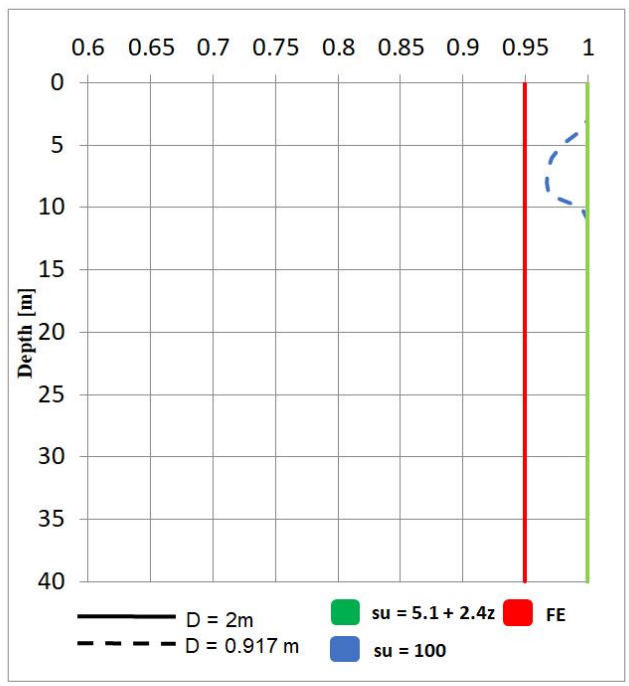

(d) $\frac{S}{D} = 5$

Figure 4.32: Comparison of p-multiplier with existing method 3-pile group (120°). With gap

4.6 4-pile group

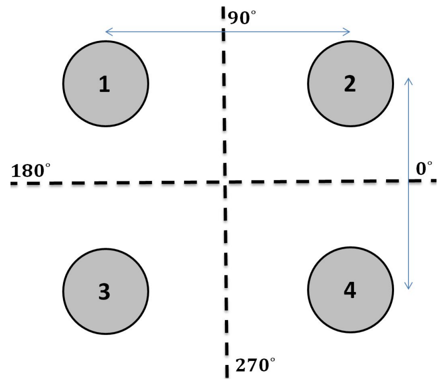

Figure 4.33: 4-pile group

4.6.1 Results

Figure 4.34 shows the resulting p-multipliers for the piles. The p-multiplier increase with S/D and is close to unity (0.97) for S/D = 5. Note that the average group p-multiplier is constant for all loading values of ω

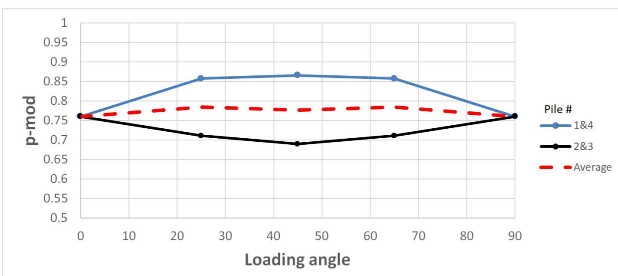

(a) $\frac{S}{D}$=2

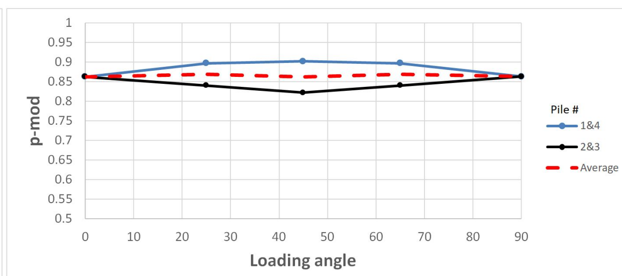

(b) $\frac{S}{D}$=3

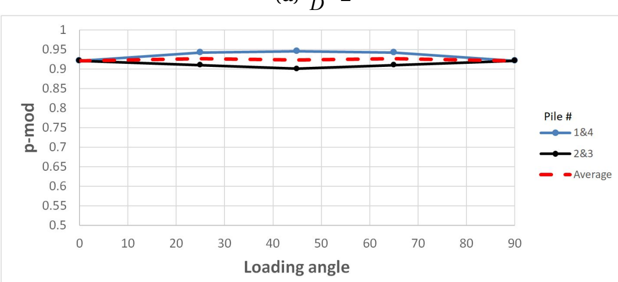

(c) $\frac{S}{D}$=4

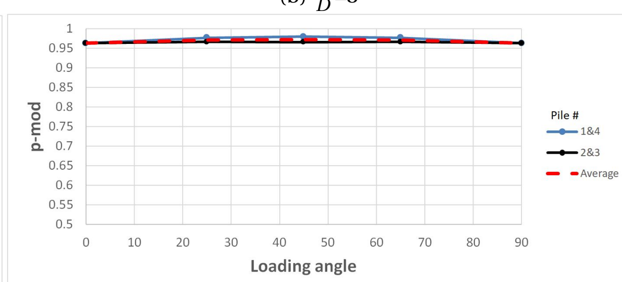

(d) $\frac{S}{D}$=5

Figure 4.34: P-multiplier for 4-pile group (S/D = 2,3,4,5)

Figure 4.35 shows the resulting y-modifier for the pile group. The pile group stiffness increase with S/D. Because the pile group has two pairs of symmetry lines with equal angles spanning them the stiffness response is not very sensitive to the loading direction.

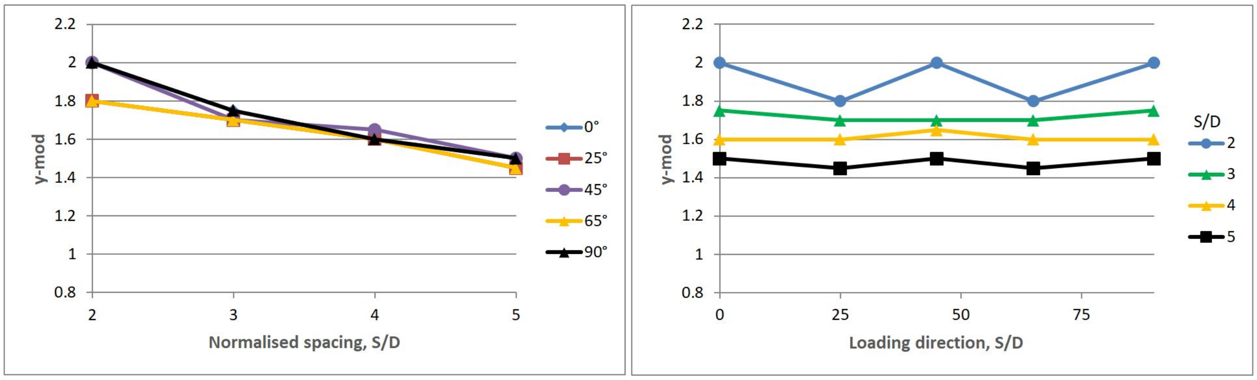

(a) Variation of y-multiplier with pile spacing

(b) Variation of y-multiplier with loading direction

Figure 4.35: fig:y-multiplier 4pile group

4.6.2 Functions for Determining Group p- and y-multipliers

The proposed function for determining the p- and y-multiplier is pesented in Table 4.5. The proposed function for the group p-multiplier (dashed lines) is compared with the FE results in Figure 4.36. The red dots are the average of the average of the p-multiplier from Figure 4.34 for different S/D.The proposed function for the y-multiplier (dashed lines) is compared with the group y-multiplier from the FE results (dots) in Figure Figure 4.37.

Table 4.5: Functions for p- and y-multipliers 4-pile group

p_{mod} A$\|\sin B\|$+C	y_{mod} a$\|\sin b\|$+c
$A = 0.065\frac{S}{D} + 0.65$	$a = -0.15\frac{S}{D} + 2.25$
$B = \pi/2$	b=$\pi/2$
$C = 0$	c=0

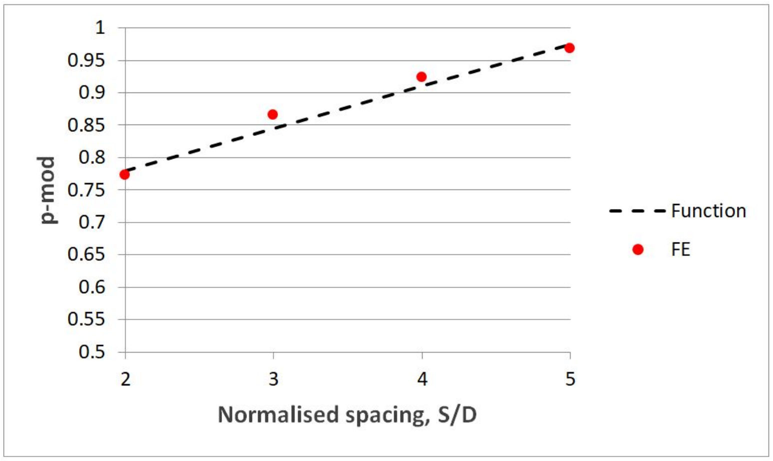

Figure 4.36: Proposed function for p_{mod} (dashed lines) vs FE results (dots)

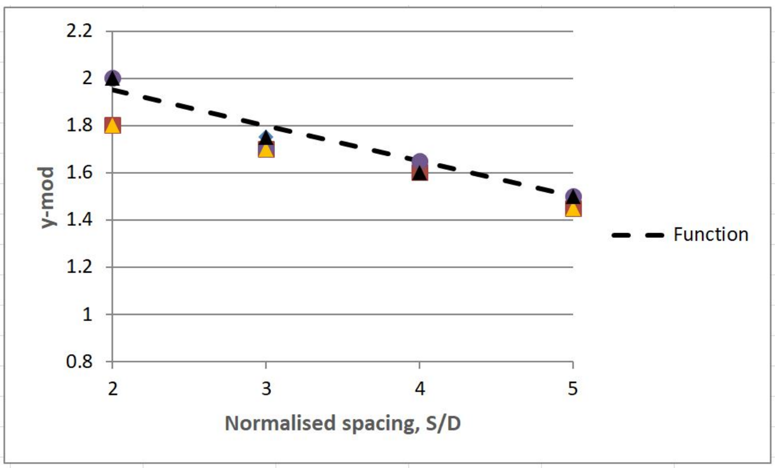

Figure 4.37: Proposed function for y_{mod} (dashed lines) vs FE results (dots)

4.6.3 Comparison with existing method

Figure 4.38 and Figure 4.39 shows the comparison with existing method for suction and no suction conditions, respectively.

With gap the existing method is generally more conservative for S/D = 2 and S/D = 3. For S/D = 4 the existing method is only more conservative for the overconsolidated soil. With no gap the FE results are more conservative for S/D ≥ 2.

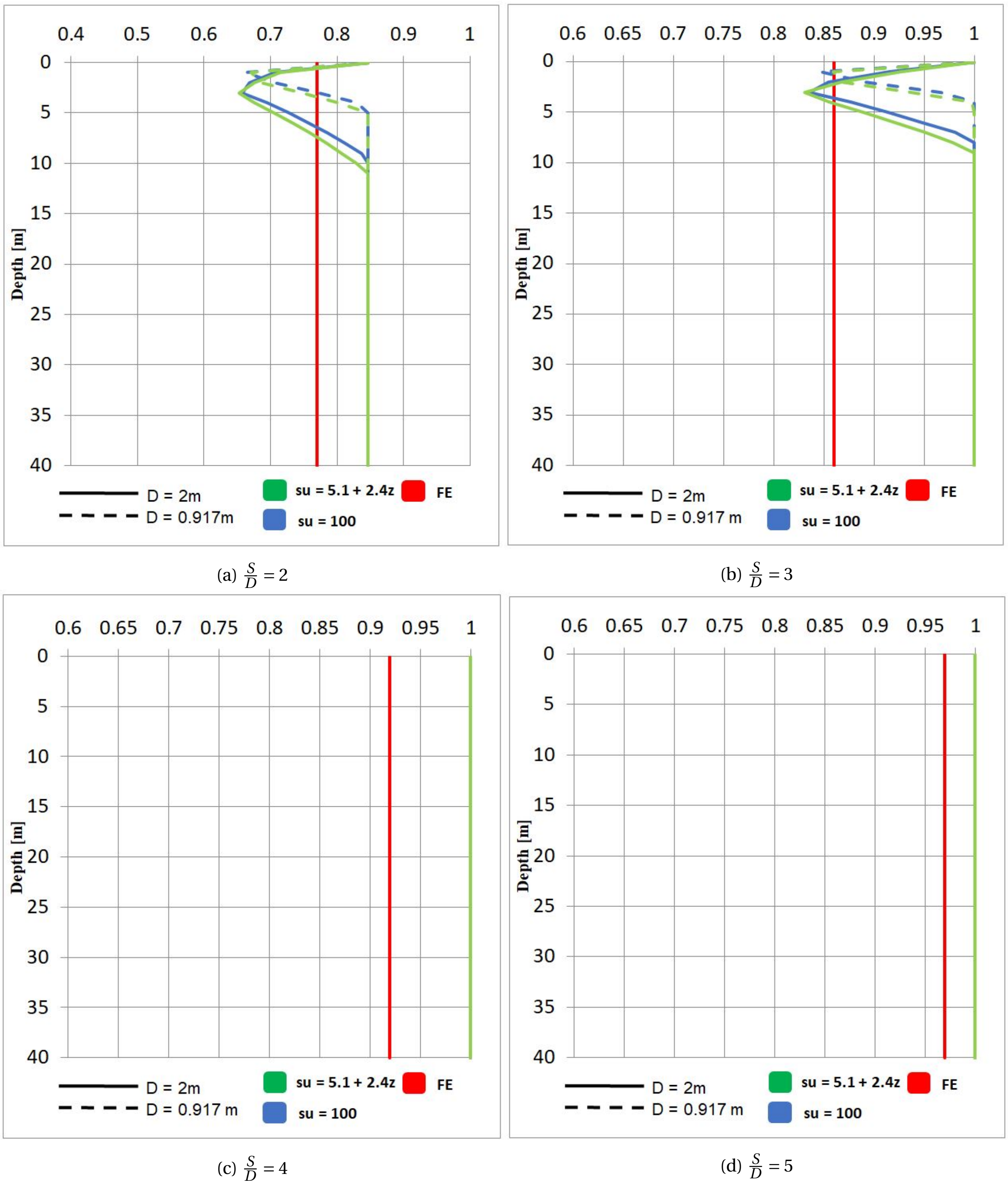

Figure 4.38: Comparison of p-multiplier with existing method 4-pile group. No gap

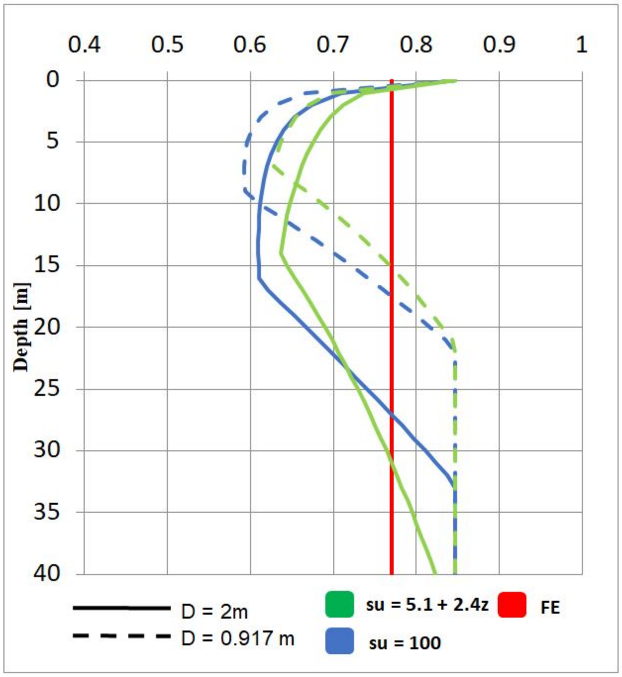

(a) $\frac{S}{D} = 2$

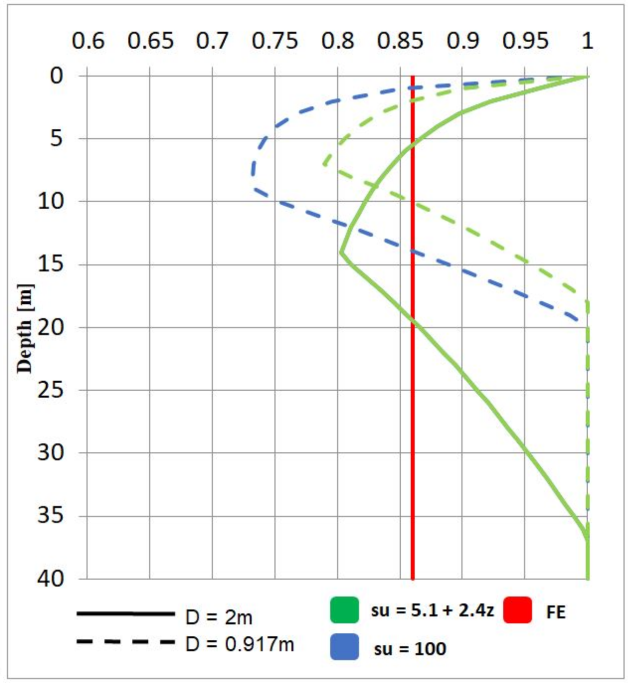

(b) $\frac{S}{D} = 3$

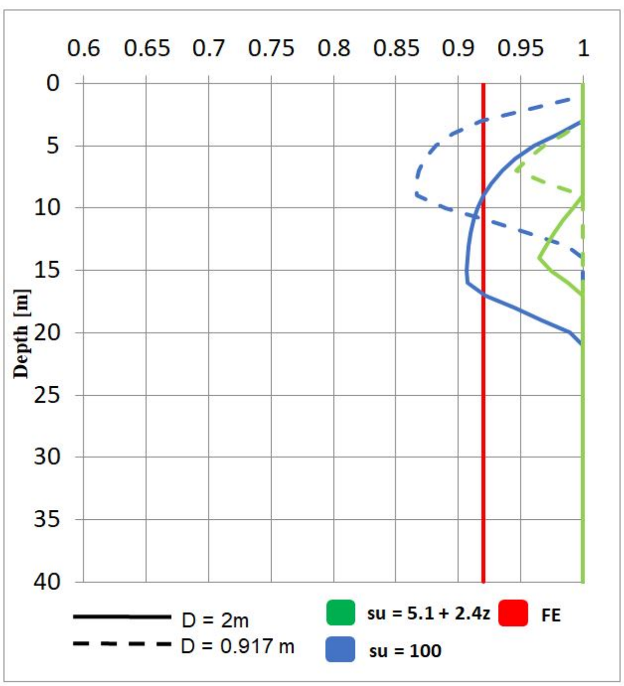

(c) $\frac{S}{D} = 4$

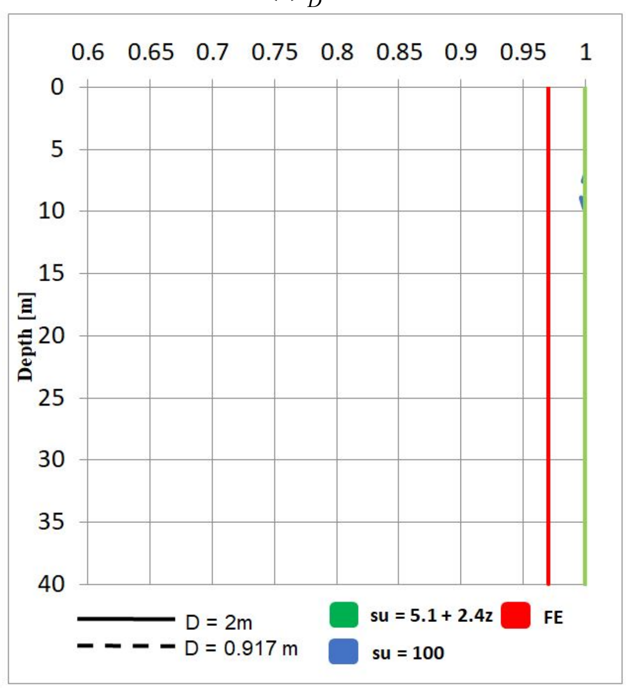

(d) $\frac{S}{D} = 5$

Figure 4.39: Comparison of p-multiplier with existing method 4-pile group. With gap

Chapter 5

Summary and Conclusions

This thesis aimed to study and quantify group effects from lateral loading of several small pile group configurations that are common for supporting offshore jacket platforms. Whereas much of the previous studies have focused on larger pile group, the results from this thesis work provide better information to engineers in design of small pile groups for jacket platforms. Group effects were studied by performing finite element analyses of a flow-around mechanism in ABAQUS with focus on pile spacing and loading direction. Expressions for predicting p- and y-multipliers based on loading angle and pile spacing has been developed. A summary of the proposed functions are given in Table 5.1.

Based on the results it can be concluded that the pile spacing has a big impact on the average group p-multiplier for all pile group configurations. The p-multiplier varies between 0.72 and 0.85 for S/D = 2, but for S/D = 5 the p-multiplier is close to unity for all pile groups, indicating that shear zone overlapping diminish with increased spacing. The loading direction only significantly affects the average group p-multiplier for pile group configurations with a relative angle between the piles greater than 90° (i.e the 2-pile group and 3-pile group (120° triangle). For these pile groups the extent of shear zone overlapping between the piles are more dependent on the loading direction and the effect of loading direction therefore becomes significant. The group y-multiplier is generally more sensitive to the loading direction than pile spacing, expect for the 4-pile group and 3-pile (equilateral) group. These two pile groups have several axes of symmetry which make the response less dependent on the loading direction. Even for large pile spacing the y-multiplier is considerably larger than unity for most pile configurations. This is in contrast to the p-multiplier and indicates that although the ultimate lateral capacity of the soil is not affected the stiffness may still be slightly reduced.

The p-multipliers from this study has been compared with the NGI approach for determining p-multipliers. The most notable findings from the comparison is that the existing approach generally predicts unnecessarly conservative p-multipliers for S/D = 2 and S/D = 3, expect for the 2-pile group. There are significant deviations between the two methods for several pile groups and spacings which shows possibilities for more optimized design in future projects. The existing approach predict less conservative p-multipliers for a no gap condition compared with a gap condition and the finite element results are generally more conservative compared to the existing method for larger pile spacings for a no gap condition.

Further work should aim to study a pile group with full penetration depth to assess whether the p- and y-multiplier vary with depth or differ between the wedge- and flow around failure.

Table 5.1: Summary of proposed design expressions for all pile groups

Summary of Design Functions		
Pile group configuration	p_{mod} A$\lvert\sin B\rvert$+C	y_{mod} a$\lvert\sin b\rvert$+c
	A = $0.033\left(\frac{S}{D}\right)^2 - 0.3\left(\frac{S}{D}\right) + 0.7$ B = ω C = $-0.023\left(\frac{S}{D}\right)^2 + 0.24\frac{S}{D} + 0.36$	a = -0.75 b = ω c = 1.75
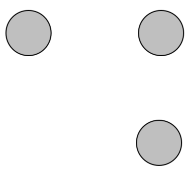	A = $0.05\frac{S}{D}$ B = $\pi/2$ C = 0.75	$a = -0.065\frac{S}{D} + 0.80$ $b = \omega - \pi/4$ c=1.1
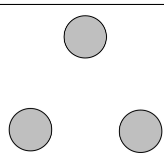	A = $0.050\frac{S}{D}$ B = $\pi/2$ C = 0.75	a=0 b=0 c=1.5
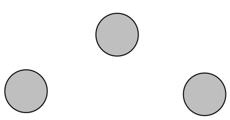	$A = 0.317 - 0.054\frac{S}{D}$ $B = \omega$ $C = 0.072\frac{S}{D} + 0.58$	a = $\begin{cases} 0.3, & S/D = 2, \\ 0.5, & S/D > 2. \end{cases}$ b=ω-$\pi/2$ a = $\begin{cases} 1.4, & S/D = 2, \\ 1.1, & S/D > 2. \end{cases}$
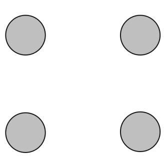	$A = 0.065\frac{S}{D} + 0.65$ $B = \pi/2$ $C = 0$	$a = -0.15\frac{S}{D} + 2.25$ b=$\pi/2$ c=0

Bibliography

Abbas Al-Shamary, J. M., Chik, Z., and Taha, M. R. (2018). Modeling the lateral response of pile groups in cohesionless and cohesive soils. *International Journal of Geo-Engineering*, 9(1):1.

Al-Jubair, H. S. and Abbas, S. A. (2014). Finite element analyses of laterally loaded pile groups in um qaser port. *International Journal of Scientific Engineering Research*, 5(11):662–668.

Alkloub, A., Allouzi, R., Alkloub, H., and Al-Ajarmeh, R. (2018). A full 3-d finite element analysis of group interaction effect on laterally loaded piles. *Modern Applied Science*, 12(5).

Allahverdizadeh, P. (2015). Group effects on piles behavior under lateral loading. *Proceedings of the International Foundations Congress and Equipment Expo 2015*, pages 1142–1151.

API (2014). Geotechnical and foundation design considerations. *American Petroleum Institute*.

Bogard, D. and Matlock, H. (1983). Procedures for analysis of laterally loaded pile groups in soft clay. *Proc. of Conference on Geotechnical Engineering*, pages 499–535.

Brown, D. A., Morrison, C., and Reese, L. C. (1988). Lateral load behavior of pile group in sand. *Journal of Geotechnical Engineering*, 114(11):1261–1276.

Brown, D. A., O'Neill, M., Hoit, M. I., McVay, M. C., Naggar, M. H. E., and Chakraborty, S. (2001). Static and dynamic lateral loading of pile groups. Report, National Cooperative Highway Research Program.

Brown, D. A., R. L. C. and O'Neill, M. W. (1987). Cyclic lateral loading of a large scale pile group. *ASCE Journal of Geotechnical Engineering*, 113(11):1326–1343.

Budiman, J. and Ahn, K. (2005). *Effects of Pile Cap in Single Pile and Lateral Capacity of Pile Group*, pages 1–16.

Chandrasekaran, S. S., Boominathan, A., and Dodagoudar, G. R. (2010). Group interaction effects on laterally loaded piles in clay. *Journal of Geotechnical and Geoenvironmental Engineering*, 136(4):573–582.

Christensen, D. S. (2006). *Full Scale Static Lateral Load Test of a 9 Pile Group in Sand*. Thesis.

DNV (2017). Offshore soil mechanics and geotechnical engineering. Report, Det Norske Veritas.

Dodds, A. M. and Martin, G. R. (2007). *Modeling Pile Behavior in Large Pile Groups Under Lateral Loading*.

Fayyazi, M. S. (2015). *Numerical Study on the Response of Pile Groups Under Lateral Loading*. Thesis.

Fayyazi, M. S., Taiebat, M., and Finn, W. D. L. (2014). Group reduction factors for analysis of laterally loaded pile groups. *Canadian Geotechnical Journal*, 51(7):758–769.

Focht Jr, J. A. and Koch, K. J. (1973). Rational analysis of the lateral performance of offshore pile groups. *Offshore Technology Conference*, pages 701–708.

Grimstad, G., Andresen, L., and Jostad, H. P. (2012). Ngi-adp: Anisotropic shear strength model for clay. *International Journal for Numerical and Analytical Methods in Geomechanics*, 36(4):483–497.

Hetenyi, M. (1946). *Beams of Elastic Foundation*. University of Michigan Press. University of Michigan Press, Ann Arbor, MI.

Huang, A.-B., Hsueh, C.-K., O'Neill, M. W., Chern, S., and Chen, C. (2001). Effects of construction on laterally loaded pile groups. *Journal of Geotechnical and Geoenvironmental Engineering*, 127(5):385–397.

Ilyas, T., Leung, C. F., Chow, Y. K., and Budi, S. S. (2004). Centrifuge model study of laterally loaded pile groups in clay. *Journal of Geotechnical and Geoenvironmental Engineering*, 130(3):274–283.

ISO (2014). Petroleum and natural gas industries — specific requirements for offshore structures. Report, International Organization for Standardization.

Jeanjean, P. (2009). Re-assessment of py curves for soft clays from centrifuge testing and finite element modeling. *Offshore Technology Conference*, page 23.

Jeanjean, P., Zhang, Y., Zakeri, A., Andersen, K., Gilbert, R., and Senanayake, A. (2017). A framework for monotonic py curves in clays. *Offshore Site Investigation Geotechnics 8th International Conference Proceeding*, 108(141):108–141.

Kagawa, T. (1992). Modeling soil reaction to laterally loaded piles. *Transportation Research Record 1336*, page 8.

Karasin, A. and Aktas, G. (2014). An approximate solution for plates resting on winkler foundation. *Inational Journal of Civil Engineering and Technology*, 5:114–124.

Matlock, H. (1970). Correlation for design of laterally loaded piles in soft clay. *Offshore Technology Conference*, pages 577–607.

McClelland, B. and Focth, A. J. J. (1956). Soil modulus of laterally loaded piles. *Journal of the Soil Mechanics and Foundations Division*, 82(4):1–24.

McVay, M., Casper, R., and Shang, T.-I. (1995). Lateral response of three-row groups in loose to dense sands at 3d and 5d pile spacing. *Journal of Geotechnical Engineering*, 121(5):436–441.

McVay, M., Zhang, L., Molnit, T., and Lai, P. (1998). Centrifuge testing of large laterally loaded pile groups in sands. *Journal of Geotechnical and Geoenvironmental Engineering*, 124(10):1016–1026.

Meimon, Y., B. F. and Jezequel, J. F. (1986). Pile group behaviour under long time lateral monotonic and cyclic loading. *Numerical Methods in Offshore Piling : Proceedings of the 3rd International Conference*, pages 285–302.

Morrison, C. and Reese, L. C. (1988). Lateral-loadtest of a full-scale pile group in sand. Report, U.S. Army Engineer Waterway Experiment Station.

Murff, J. D. and Hamilton, J. M. (1993). P-ultimate for undrained analysis of laterally loaded piles. *Journal of Geotechnical Engineering*, 119(1):91–107.

Muskulus, M. and Schafhirt, S. (2014). Design optimization of wind turbine support structures-a review. *Journal of Ocean and Wind Energy*, 1(1):12–22.

Nichols, N. W., MJ, R., Mukherjee, K., Ayob, B., Sapihie, M., Clausen, C. J., and Lunne, T. (2014). Effect of lateral soil strength and stiffness on jacket foundation integrity and design for south china sea sites. *Offshore Technology Conference-Asia*.

O'Neill, M. and Murchison, J. M. (1983). An evaluation of py relationships in sands. a report to the american petroleum institute. *Houston, TX, USA: University of Houston*.

Pando, M. A., Ealy, C. D., Filz, G. M., Lesko, J., and Hoppe, E. (2006). A laboratory and field study of composite piles for bridge substructures. Report, FHWA.

Poulos, H. G. and Davis, E. H. (1980). *Pile Foundation Analysis and Design*. Series in Geotechnical Engineering. Wiley.

Randolph, M. F. and Houlsby, G. (1984). The limiting pressure on a circular pile loaded laterally in cohesive soil. *Geotechnique*, 34(4):613–623.

Reese, L. C. (1957). Discussion on soil modulus of laterally loaded piles. *Journal of the Soil Mechanics and Foundations Division*, 83(2):1228–21–1228–34.

Reese, L. C., Cox, W. R., and Koop, F. D. (1975). Field testing and analysis of laterally loaded piles in stiff clay. *Offshore Technology Conference*, page 10.

Reese, L. C. and van Impe, W. (2010). *Single Piles and Pile Groups Under Lateral Loading*. CRC Press, 2 edition.

Rollins, K. M., Lane, J. D., and Gerber, T. M. (2005). Measured and computed lateral response of a pile group in sand. *Journal of Geotechnical and Geoenvironmental Engineering*, 131(1):103–114.

Rollins, K. M., Olsen, K. G., Jensen, D. H., Garrett, B. H., Olsen, R. J., and Egbert, J. J. (2006). Pile spacing effects on lateral pile group behavior: Analysis. *Journal of Geotechnical and Geoenvironmental Engineering*, 132(10):1272–1283.

Rollins, K. M., Peterson, K. T., and Weaver, T. J. (1998). Lateral load behavior of full-scale pile group in clay. *Journal of Geotechnical and Geoenvironmental Engineering*, 124(6):468–478.

Rollins, K. M. and Sparks, A. (2002). Lateral resistance of full-scale pile cap with gravel backfill. *Journal of Geotechnical and Geoenvironmental Engineering*, 128(9):711–723.

Ruesta, P. F. and Townsend, F. C. (1997). Evaluation of laterally loaded pile group at roosevelt bridge. *Journal of Geotechnical and Geoenvironmental Engineering*, 123(12):1153–1161.

Snyder, J. L. (2004). *Snyder, J.L. 2004. Full-scale lateral load tests of a 3 × 5 pile group in soft clays and silts. Master's thesis, Brigham Young University.* Thesis.

Walsh, J. M. (2005). *Full-scale Lateral Load Test of a 3x5 Pile Group in Sand.* Thesis.

Winkler, E. (1867). *Die Lehre von der Elastizität und Festigkeit.* Dominicus Verlag, Prag.

Yu, J., Huang, M., and Zhang, C. (2015). Three-dimensional upper-bound analysis for ultimate bearing capacity of laterally loaded rigid pile in undrained clay. *Canadian Geotechnical Journal*, 52(11):1775–1790.

Zhang, Y. and Andersen, K. H. (2017). Scaling of lateral pile p-y response in clay from laboratory stress-strain curves. *Marine Structures*, 53:124–135.

Zhang, Y., Andersen, K. H., and Tedesco, G. (2016). Ultimate bearing capacity of laterally loaded piles in clay – some practical considerations. *Marine Structures*, 50:260–275.

NTNU
Norwegian University of
Science and Technology